固相における置換ポリアセチレンの外部刺激による ヘリックス転移

Doctoral Thesis

Helix Rearrangement of Substituted Polyacetylenes Induced by External Stimulus in the Solid Phase

ASAHI MOTOSHIGE

Department of Chemical and Materials Engineering

Muroran Institute of Technology

博 士 学 位 論 文

題　目

固相における置換ポリアセチレンの外部刺激によるヘリックス転移

氏　名　　元茂　朝日

室蘭工業大学　大学院工学研究科

博士後期課程　物質工学専攻

Contents

Introduction 1

Chapter 1. Irreversible Helix Rearrangement from *Cis-transoid* to *Cis-cisoid* in Poly (*p-n*-hexyloxyphenylacetylene) Induced by Heat-treatment in Solid Phase 11

Chapter 2. *Contracted Helix* to *Stretched Helix* Rearrangement of an Aromatic Polyacetylene Prepared in *n*-Hexane with $[Rh(norbornadiene)Cl]_2$-triethylamine Catalyst 40

Chapter 3. Synthesis and Solid State *Helix* to *Helix* Rearrangement of Poly(phenylacetylene) Bearing *n*-Octyl Alkyl Side Chains 68

Summary of this thesis 100

List of publications 104

Acknowledgments 106

Introduction

π-Conjugated Polymers

π-Conjugated polymers consist of alternative double-bonds and single-bonds, and they have been synthesized using various catalysts.[1,2] Furthermore, at present their chemical and physical properties are also studying extensively.[1] There are two types of π-conjugation polymers. The first is linear π-conjugated polymers such as poly(acetylene)s,[3] poly(phenylene)s,[4] poly(thiophene)s,[5] and another is poly(aromatic hydrocarbon)s such as graphite hexa-*peri*-hexabenzocoronenes.[6]

These polymers have fairly long π-conjugation lengths which affect the various properties, e.g., colors such as yellow, red, and black.[7,8] These phenomena were caused by the degree of the π-conjugation system. The differences or changes of polymer colors are correlated with the absorption band depending on conformation of the π-conjugated main-chains or phenyl-rings.

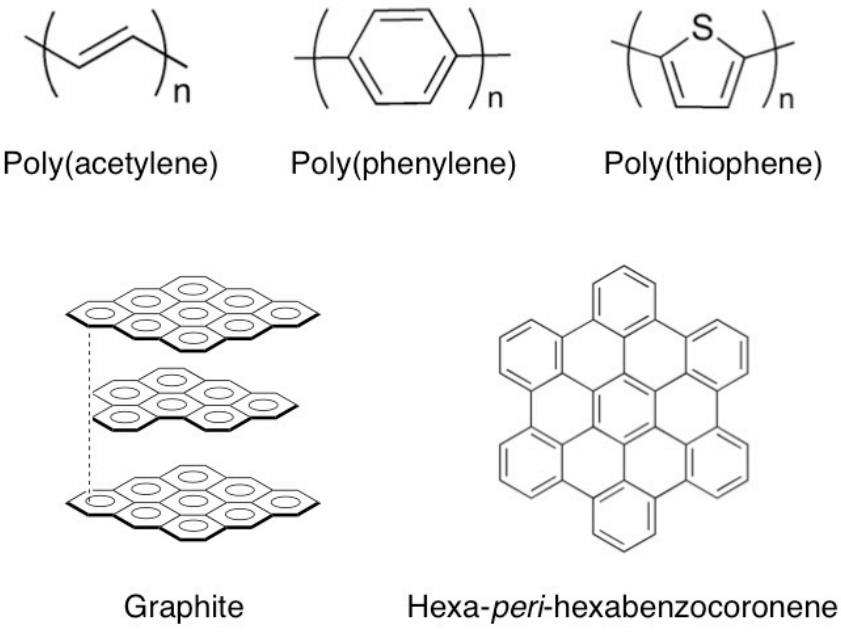

Figure 1. Various of π-conjugated polymers and materials.

Polyacetylenes

Polyacetylene is one of typical π-conjugated polymers which have alternative single bond and double bond. In 1958, Natta and coworkers prepared the poly(acetylene)s for the first time by using a Ti-based catalyst.[9] This polyacetylene is known to have a *trans-transoid* structure among four theoretically possible conformers, e.g., *cis-transoid*, *cis-cisoid*, *trans-cisoid*, and *trans-transoid*.[10]

Films of the non-substituted polyacetylene were synthesized by Shirakawa and his colleagues. Then, they found that the electrical conductivity is highly increased by halogen doping.[11] This is a very important finding in the field of chemistry. Because this is a first discover, i.e., the polyacetylene polymers have high industrial potential as indicated by high conductivity as metals. Moreover, this work provided the Nobel Prize award in Chemistry for Prof. ALAN J. HEEGER, Prof. ALAN G. MACDIARMID, and Prof. HIDEKI SHIRAKAWA in 2000. Although this non-substituted polyacetylene has important and interest properties but this polymer has also disadvantages, e.g., insoluble in organic solvents. On the other hands, many substituted polyacetylenes have displayed interesting properties, such as oxygen permeability,[12] semi conductivities,[13] humidity sensitivity,[14] nonlinear optical properties (NLO),[15] amino acid permselective properties,[16] external stimulus responsibility,[17] anti-ferromagnetic properties accompanying with the time memory effect,[18] and radiation sensitive properties.[19] The substituted polyacetylenes having many kind of substitutes as the side-chain have been synthesized by using various type of catalysts such as Ziegler-Natta catalyst, $Fe(acac)_3$-$AlH(i\text{-}Bu)_2$,[20] Luttinger catalyst,

(n-$Bu_3P)_2NiCl_2$-$NaBH_4$,[21] $Co(NO_2)_2$-$NaBH_4$,[22] $RhCl_3$-$LiBH_4$,[20] Wilkinson catalyst, $RhCl(PPh_3)_3$,[20] Pt or Ni complex catalysts,[23,34] metathesis catalysts such as WCl_6 or $MoCl_5$,[24,25] Rh complex catalyst like $[Rh(nbd)Cl]_2$-cocatalyst (nbd=norbornadiene),[26] and zwitterionic Rh catalyst.[27] Especially, metathesis catalysts have been developed by some groups.[24,25] It is well known that the transition metal chloride-based catalysts are effective in metathesis polymerization of substituted acetylenes, but the molecular weight is up to around 5000. In 1974, Masuda group found that transition metal chlorides, i.e., WCl_6 and $MoCl_5$, are quite active for the polymerization of substituted acetylene.[28] However, the molecular weight of the polymers is less than 10000. Additionally, these polymers had different structures, e.g., *cis*-rich or *trans*-rich whose structures are depended on polymerization conditions or catalysts, and these were soluble and mainly amorphous.[29]

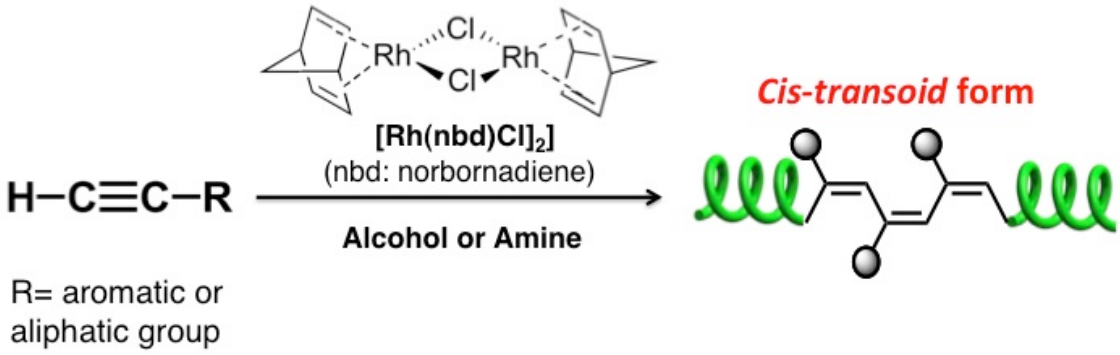

Figure 2. Synthesis of substituted polyacetylene with a Rh complex catalyst.

The $[Rh(nbd)Cl]_2$ catalyst was revealed to induce the polymerization of the substituted acetylenes under quite mild conditions by Tabata group.[26] And also, the Rh

complex catalyst afford the highly stereoregular substituted polyacetylenes with a helical *cis-transoid* main-chain which generates a molecular assemble in the solid phase, i.e., pseudohexagonal crystal structure called columnar which has a long-range positional order along the molecular axis.[30] Tabata group also revealed that triethylamine or alcohol causes the dissociation of the binuclear complex, $[Rh(nbd)Cl]_2$ into the monomeric species which may, in turn, function as an important initiation species for this polymerization. There are marked structural and physicochemical differences between π–conjugated polymers prepared using Rh complex and metathesis catalysts as evidenced by NMR, ESR, and laser Raman spectroscopies.[26,30]

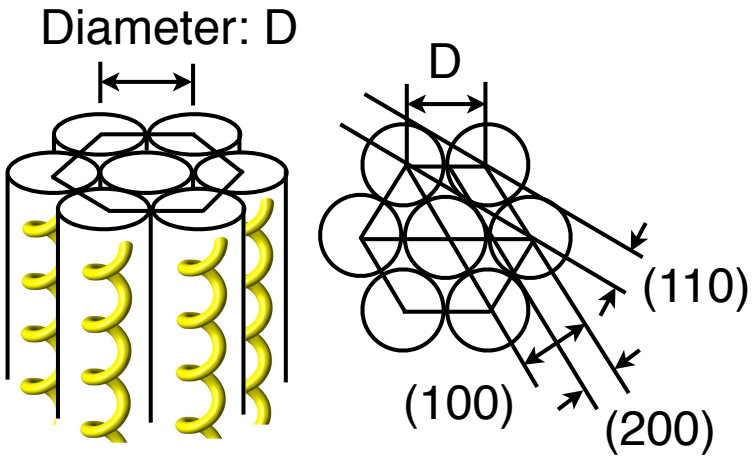

Figure 3. Pseudohexagonal crystal structure called columnar.

Helical Polyacetylenes

Deoxyribonucleic acid (DNA) has a stable helical conformation. Many helical

polymers as DNA have been synthesized. Recently, helical polymers including substituted polyacetylenes with one-handed helical conformation have received much attention because the chiral structure are expected to enhance unique properties and properties.[31] For example, Aoki's group have reported helix-sense-selective polymerization of achiral phenlacetylene monomers having two hydroxyl groups.[32] Yashima's group has been reported the helix inversions of various helical polyacetylenes proposed based on CD spectral data.[31,33]

On the other hands, Tabata's group reported that poly(phenylacetylene)s prepared using the Rh complex catalyst showed various colors, e.g., red, yellow, and black.[17] These colors in difference are related to different π-conjugated system. Accordingly, it is considered that the main-chain of these polymers have different pitches, loose helix or tight helix.

Purposes of this Thesis

The substituted polyacetylenes display many interesting properties which are related to the geometrical structure and higher-order structure of the helical main-chain. However, the helical pitch width, its diameter, and the crystal structures of substituted polyacetylenes which were stereoregularly prepared with the Rh complex catalyst, $[Rh(norbornadiene)Cl]_2$-triethylamine have not yet been investigated in detail. Therefore, we have investigated whether the geometrical and helical structures of the substituted polyacetylenes can be controlled through molecular design and/or external stimuli.

Reference

1. H. S. Nalwa, E.d. Handbook of Organic Conductive Molecules and Polymers, Wiley, Chichester **1997**.
2. M. P. Stevens, Polymer Chemistry an Introduction, Oxford University Press, Oxford, **1999**.
3. A. Furlani, P. Biev, M. V. Russo, M. Fiorentio, *Gazz. Chim. Ital.* **1987**, 107, 373.
4. (a) P. Kovacic, A. Kyriakis, *J. Am. Chem. Soc.* **1963**, 85, 454. (b) J. H. Burroughes, D. D. C. Bradley, A. R. Brown, R. N. Marks, K. Mackay, R. H. Friend, P. L. Burn, A. B. Holmes, *Nature* **1990**, 347-539.
5. H. Sirringhuas, *Adv. Mater* **2005**, 17, 2411.
6. S. Ito, M. Wehmeier, J. D. Brand, C. Kübel, R. Epsch, J. P. Rabe, K. Müllen, *Chem. Eur. J.* **2000**, 6. 4327-4342.
7. Y. Mawatari, M. Tabata, *J. Jpn. Soc. Colour Mater* **2009**, 82, 204-209.
8. I. F. Perepichka, D. F. Perepichka, H. Meng, F. Wudl, *Adv. Mater.* **2005**, 17, 2281-2305.
9. G. Natta, G. Mazzanti, P. Corradini, *Atti Acad Naz. Lincei, Cl. Sci. Fis. Mat. Nat. Rend.* **1958**, 8, 25: 3.
10. M. Tabata, Y. Inada, K. Yokota, Y. Nozaki, *J. Macromol. Sci., Pure Appl. Chem.*, **1994**, A31, 465.
11. H. Shirakawa, E. G. Louis, A. G. Macdiarmid, C. K. Chiang, A. G. Heeger, *J. Chem. Soc., Chem. Comm.* **1977**, 578-580.
12. T. Masuda, E. Isobe, T. Higashimura, K. Takada, *J. Am. Chem. Soc.* **1983**, 105,

7473-7474.

13. (a) T. A. Skotheim, Ed. Handbook of Conducting Polymers; Dekker: New York, **1986**, vol. 1-2. (b) J. R.Ferraro, J. M. Williams, Eds. Introduction to Synthetic Electrical Conductors; Acad. Press Inc: New York **1987**. (c) J. C. Salomone, Ed. Polymeric Materials; CRC Press: New York **1996**, vol. 8, 6481.
14. (a) A. Asdente, A. Ottoboni, A. Furlani, M. V. Russo, Chemtronics **1991**, 5, 75-80. (b) A. Furlani, G. Iucci, M. V. Russo, A. Bearzotti, R. D'Amico, Sens Actuators B **1992**, B7, 447-450.
15. (a) D. Neher, A. Wolf, C. Bubeck, G. Wegner, *Chem. Phys. Lett.* **1989**, 163, 116-122. (b) J. L. Bredas, C. Adant, P. Tacks, A. Persoons, M. Pierce, *Chem. Rev.* **1994**, 94, 243-278. (c) M. Falconieri, R. D'Amato, M. V. Russo, A. Furlani, *Nonlinear Opt.* **2001**, 27, 439-442. (c) M. Tabata, T. Sone, K. Yokota, T. Wada, H. Sasabe, *Nonlinear Opt.* **1999**, 22, 341-344. (d) T. Wada, L. Wang, H. Okawa, T. Masuda, M. Tabata, M. Wan, M. Kakimoto, Y. Imai, H. Sasabe, *Mol. Cryst. Liq. Cryst.* **1997**, 294, 245-250.
16. (a) T. Aoki, K. Shinohara, E. Oikawa, *Chem. Lett.* **1993**, 22, 2009-2012. (b) M. Teraguchi, J. Suzuki, T. Kaneko, T. Aoki, T. Masuda, *Macromolecules* **2003**, 36, 9694-9697. (c) Y. Suzuki, J. Tabei, M. Shiotsuki, Y. Inai, F. Sanda, T. Masuda, *Macromolecules* **2008**, 41, 1086-1093. (d) E. Yashima, Y. Maeda, Y. Okamoto, *J. Am. Chem. Soc.* **1998**, 120, 8895-8896. (e) E. Yashima, T. Matsushima, Y. Okamoto, *J. Am. Chem. Soc.* **1997**, 119, 6345-6359. (f) R. Nonokawa, E. Yashima, *J. Am. Chem. Soc.* **2003**, 125, 1278-1283.

17. Y. Mawatari, M. Tabata, *J. Jpn. Soc. Colour Mater* **2009**, 82, 204-209.

18. (a) Y. V. Korshak, T. V. Medvedeva, A. A. Ovchinnikov, V. Spector, *Nature* **1987**, 326, 370-372. (b) N. Tyutyulkov, K. Müllen, M. Baumgarten, A. Ivanova, A. Tadjer, *Synth. Met.* **2003**, 139, 99-107. (c) M. Tabata, Y. Nozaki, W. Yang, K. Yokota, Y. Tazuke, *Proc. Jpn. Acad.* **1995**, 71, 219-224. (d) K. H. Fisher, J. A. Herz, Spin glass; Cambridge University Press: **1991**, 30. (e) J. J. Pregjean, J. Souletie, *J. Phys.* **1980**, 41, 1335-1352. (f) L. Floch, F. Hammann, J, Ocio, M. Vincent, *Euro. Phys. Lett.* **1992**, 18, 647-652. (g) D. G. Xenikos, H. Multer, C. Jouan, A. Suilpice, J. L. Tholence, *Solid. State. Commun.* **1997**, 102, 681-685. (h) M. Tabata, Y. Watanabe, S. Muto, *Macromol. Chem. Phys.* **2004**, 205, 1174-1178. (i) Y. Watanabe, S. Muto, M. Tabata, *Jpn. J. Appl. Phys. Part 2 Lett.* **2004**, 43, 300-302.

19. M. Kozuka, T. Sone, M. Tabata, Y. Sadahiro, T. Enoto, *Radiation Phys. Chem.* **2002**, 63, 59-61.

20. R. J. Kern, *J. Polym. Sci., Polym. Chem. Ed.* **1969**, 7, 621-631.

21. L. B. Luttinger, *J. Org. Chem.* **1962**, 27, 1591-1596.

22. F. D. Kleist, N. R. Byrd, *J. Polym. Sci: Polym. Chem. Ed.* **1969**, 7, 3419.

23. P. Biev, A. Furlani, M. V. Russo, *Gazz. Chim. Ital.* **1980**, 110, 25.

24. A. Furlani, P. Biev, M. V. Russo, A. Fiorentio, *Gazz. Chim. Ital.* **1987**, 117, 373.

25. T. Masuda, T. Higashimura, *Adv. Polym. Sci.* **1986**, 81, 121-165.

26. (a) M. Tabata, W. Yang, K. Yokota, *Polym. J.* **1990**, 22, 1105-1107. (b) W. Yang, M. Tabata, K. Yokota, *Polym. J.* **1991**, 23, 1135-1138. (c) M. Tabata, W. Yang, K. Yokota, *J. Polym. Sci. Part A: Polym. Chem.* **1994**, 32, 1113-1120. (d) Y. Yoshida,

Y. Mawatari, C. Seki, T. Hiraoki, H. Matsuyama, M. Tabata, *Polymer* **2011**, 52, 646-651.

27. (a) Y. Kishimoto, P. Eckerle, T. Miyataka, M. Kainosho, A. Ono, T. Ikariya, R. Noyori, *J. Am. Chem. Soc.* **1999**, 121, 12035-12044. (b) N. Onishi, M. Shiotsuki, F. Sanda, T. Masuda, *Macromolecules* **2009**, 42, 4071-4076. (c) T. Nishimura, Y. Ichikawa, T. Hayashi, N. Onishi, M. Shiotsuki, T. Masuda, *Organometallics* **2009**, 28, 4890-4893. (d) M. Shiotsuki, N. Onishi, F. Sanda, T. Masuda, *Chem. Lett.* **2010**, 244-245. (e) M. Shiotsuki, F. Sanda, T. Masuda, *Polym. Chem.* **2011**, 2, 1044-1058.
28. T. Masuda, K. Hasegawa, T. Higashimura, *Macromolecules* **1974**, 7, 728–731.
29. Y. Fujita, Y. Misumi, M. Tabata, T. Masuda, *J. Polym. Sci., Part A: Polym. Chem.* **1998**, 36, 3157.
30. (a) M. Tabata, S. Kobayashi, Y. Sadahiro, Y. Nozaki, K. Yokota, W. Yang, *J. Macromol. Sci., Pure Appl. Chem.* **1997**, *A34*, 641-653. (b) M. Tabata, T. Sone, Y. Sadahiro, *Macromol. Chem. Phys.* **1999**, *200*, 265.
31. K. Maeda, E. Yahima, *J. Synth. Org. Chem. JPN.* **2002,** 60, 878-890.
32. T. Aoki, T. Kaneko, N. Maruyama, A. Sumi, M. Takahashi, T. Sato, M. Teraguchi, *J. Am. Chem. Soc.* **2003**, 125, 6346-6347.
33. K. Maeda, H. Mochizuki, M. Watanabe, E. Yashima, *J. Am. Chem. Soc.* **2006**, 128, 7639-7650.

Chapter 1

Irreversible Helix Rearrangement from *Cis-transoid* to *Cis-cisoid* in Poly(*p*-*n*-hexyloxyphenylacetylene) Induced by Heat-treatment in Solid Phase

Abstract

Polymerization of *p*-*n*-hexyloxyphenylacetylene(*p*HPA) by using a [Rh(norbornadine)Cl]$_2$-triethylamine catalyst was carried out at room temperature to afford stereoregular helical poly(*p*-*n*-hexyloxyphenylacetylene)s (P*p*HPAs). When ethanol and n-hexane were used as polymerization solvents, a bright yellow P*p*HPAs, poly(**Y**) with M_n = 8.5 x 10^4 and its purple red polymer, poly(**R**) with M_n = 5.3 x 10^4 were obtained in 95% yields and 84% yields, respectively. Diffuse reflective UV-vis spectra of poly(**Y**) and poly(**R**) in solid phase showed different broad absorption peaks at 445 and 575 nm, respectively. X-Ray diffraction patterns of poly(**Y**) and poly(**R**) showed typical columnar structures assignable to *cis*-*transoid* and *cis*-*cisoid* structures, respectively, which were also supported by molecule mechanics calculation. Poly(**Y**) was irreversibly transformed to a reddish-black polymer, poly(**Y**→**B**), which columnar diameter was nearly the same as that of poly(**R**). Further, poly(**Y**) showed an exothermic peak in the differential scanning calorimetry trace at 80 ℃ for 1 h in N_2 gas. Thus, these findings suggest a thermally irreversible rearrangement from an unstable *cis*-*transoid* form, poly(**Y**) with a stretched *cis*-*transoid* helix to a stable *cis*-*cisoid* form, poly(**R**), with a contracted *cis*-*cisoid* helix in the solid phase to give poly(**Y**→**B**) with the *cis*-*cisoid* form.

Introduction

Polyacetylenes (PAs) and mono-substituted PAs (SPAs), which are one of the typical conjugated polymers, have been prepared by using various types of catalysts, such as Ziegler–Natta catalyst, $Fe(acac)_3$-$AlH(i\text{-}Bu)_2$,[1] Luttinger catalyst, $(n\text{-}Bu_3P)_2NiCl_2$-$NaBH_4$,[2] $Co(NO_2)_2$-$NaBH_4$,[3] $RhCl_3$-$LiBH_4$,[1] Wilkinson catalyst, $RhCl(PPh_3)_3$,[1] Pt or Ni complex catalysts,[4,5] metathesis catalysts such as WCl_6 or $MoCl$[5,6] Rh-diene catalyst, $[Rh(nbd)Cl]_2$-cocatalyst (norbornadiene, nbd),[7] and zwitterionic mono-Rh complex catalyst.[8] Among them, the Rh catalyst was revealed to induce the polymerization of the substituted acetylenes (SAs) and afford the highly stereoregular SPAs with a helical *cis-transoid* main-chain which generates a molecular assemble based on the hexagonal crystal structure called a columnar.[7,9] The SPAs display interesting solid-phase properties, such as oxygen permeability,[10] semiconductivities,[11] humidity sensitivity,[12] nonlinear optical properties,[13] amino acid permselective properties,[14] external stimulus responsibility,[15] antiferromagnetic properties accompanying with the time memory effect,[16] and radiation sensitive properties.[17] To the best of our knowledge, the *cis-cisoid* helix with contracted pitches has been considered as an interesting one among four theoretically possible conformers, for example, *cis-transoid*, *cis-cisoid*, *trans-cisoid*, and *trans-transoid* for a long time.[18,19] Further it seems that an important question regarding whether the *cis-cisoid* helix is really generated in solution and/or in solid phase has remained still unsolved.[18] Because detailed physicochemical properties regarding the *cis-transoid* and *cis-cisoid* helices in the solid and/or solution phases are not enough understood. In this report, we

describe the formation of the two poly(*p*-*n*-hexyloxyphenylacetylene)s (P*p*HPAs), that is, a bright yellow poly(**Y**) consisting of *cis*-*transoid* helix with stretched pitches and purple red poly(**R**) consisting of *cis*-*cisoid* helix with contracted pitches. A Rh-diene catalyst, $[Rh(nbd)Cl]_2$ and triethylamine(NEt_3) as cocatalyst in ethanol (EtOH) or *n*-hexane (Hex) were used for the polymerization at 25 ℃. Furthermore, the thermally induced rearrangement of the stretched *cis*-*transoid* helical form to the contracted *cis*-*cisoid* form at about 80 ℃ was studied, and such helical structures for poly(**Y**) and poly(**R**) were characterized in details by 1H NMR, wide angle X-ray diffraction (XRD), solution and diffuse reflective UV–vis (DRUV–vis) spectra, resonance laser Raman spectra in solid phase using an Ar^+ laser and molecular mechanics (MM) calculation (MMFF94 force field).

Experimental Section

Materials

Absolute ethanol, *n*-hexane, and triethylamine were distilled before use. $[Rh(nbd)Cl]_2$ (nbd = norbornadiene) was purchased from Aldrich and used without further purification.

Monomer Synthesis

The monomer, *p*-*n*-hexyloxyphenylacetylene pHPA, was prepared according to a literature[20] and purified by distillation under reduce pressure before use. B. p.: 99 °C/22 Pa. ^{1}H NMR (500 MHz, $CDCl_3$, ppm): 7.41 (Ph-*H*, d, *J* = 8.9 Hz, 2H), 6.83 (Ph-*H*, d, *J* = 8.9 Hz, 2H), 3.95 ($PhOCH_2$, t, *J* = 6.7 Hz, 2H), 2.99 (C≡C*H*, s, 1H), 1.82-1.72 (OCH_2CH_2, m, 2H), 1.49-1.41 ($OCH_2CH_2CH_2$, m, 2H), 1.38-1.29 ($OCH_2CH_2CH_2CH_2CH_2$, m, 4H), 0.90 (CH_2CH_3, t, *J* = 7.1 Hz, 3H). ^{13}C NMR (125 MHz, $CDCl_3$, ppm): 159.51, 133.53, 114.41, 113.80, 83.75, 75.63, 68.03, 31.54, 29.10, 25.66, 22.58, 14.02. Anal. Calcd for $C_{14}H_{18}O$: C, 83.12; H, 8.97. Found: C, 83.08; H, 9.10.

Polymerization

Poly(*p*-*n*-hexyloxyphenylacetylene)s (PpHPA) were prepared by polymerization of pHPA using $[Rh(nbd)Cl]_2$ as catalyst and NEt_3 as cocatalyst in EtOH or Hex. In a typical procedure, 700 mg (3.5 mmol) of pHPA and 16 mg (3.5×10^{-2} mmol) of $[Rh(nbd)Cl]_2$, and 0.48 ml of NEt_3 (3.5 mmol) were dissolved in 17.3 mL of Hex or

EtOH in a specially designed U-shaped flask.[7] The polymerization was continued at 25 °C for 0.5 h, and quenched by adding 300 mL of methanol. The polymer obtained was filtered off, washed with methanol, followed by dynamic vacuum drying at 4 x 10^{-2} torr for 24 h.

Poly(**Y**) was obtained as a bright yellow powder (95%) by polymerization in EtOH: ^{1}H NMR (500 MHz, $CDCl_3$, ppm): 6.59 (br., 2H), 6.43 (br., 2H), 5.75 (br., 1H), 3.67 (br., 2H), 1.65 (br., 2H), 1.5-1.2 (br., 6H), 0.89 (br., 3H). ^{13}C NMR (125 MHz, $CDCl_3$, ppm): 158.15, 138.62, 135.69, 130.14, 128.73, 113.58, 67.86, 31.73, 29.40, 25.86, 22.63, 14.08. Anal. Calcd. for $C_{14}H_{18}O$: C, 83.12; H, 8.97. Found: C, 82.72; H, 9.07.

Poly(**R**) was obtained as a purple red powder (84%) by polymerization in Hex: ^{1}H NMR (500 MHz, $CDCl_3$, ppm): 6.59 (br., 2H), 6.43 (br., 2H), 5.75 (br., 1H), 3.67 (br., 2H), 1.65 (br., 2H), 1.5-1.2 (br., 6H), 0.89 (br., 3H). ^{13}C NMR (125 MHz, $CDCl_3$, ppm): 158.15, 138.63, 135.69, 130.18, 128.74, 113.59, 67.87, 31.74, 29.40, 25.86, 22.64, 14.08. Anal. Calcd. for $C_{14}H_{18}O$: C, 83.12; H, 8.97. Found: C, 82.22; H, 9.07.

Thermal Treatment

Poly(**Y**) placed at the bottom of a test tube was immersed in a pre-heated oil bath at 80 °C for 1 h under N_2. The color of poly(**Y**) was gradually changed from bright yellow to reddish black (poly(**Y**→**B**)).

Measurements

Number- and weight average molecular weights (M_n and M_w) of the polymers were

measured using JASCO GPC 900-1 equipped with two Shodex K-806L columns and RI detector. Chloroform was used as eluent at 40 ºC, and polystyrene standards (M_n = 800−1,090,000) were employed for calibration. ^{1}H (500 MHz) NMR and ^{13}C (125 MHz) NMR spectra were measured on a JEOL ECA-500 in $CDCl_3$ at room temperature. Solution and diffuse reflective UV-Vis (DRUV-Vis) spectra of the polymers were recorded on a JASCO V570 spectrophotometer equipped with an ISV-470 integrating sphere accessory. Wide angle X-ray diffraction (XRD) patterns of the polymers were recorded on a RIGAKU RINT2200 Ultima with CuK_α as a radiation source equipped with a heater with a programmable temperature controller (PTC-30). Differential scanning calorimetry (DSC) was performed on a SHIMADZU DSC-60 and traces were run in an atmosphere of N_2 at heating rate of 1 or 10 °C/min. Laser Raman spectra were measured on JASCO NR-1800S using laser light at 532 nm using samples obtained after mixing 3 mg of each polymer and 200 mg of KBr with a mortar and pestle.

Molecular Mechanics Calculation

Energetically optimal conformation of 20-mer of pHPA was deduced by molecular mechanics calculation using MMFF94 force field (Wavefunction, Inc., Spartan '04 Windows version 1.0.3).[21]

Results and Discussion

Polymerization

Polymerization of the monomer, pHPA, in a catalytic system of $[Rh(nbd)Cl]_2/NEt_3$ in EtOH or Hex was carried out at 25 °C to afford the corresponding PpHPAs as shown in Scheme 1. The yield with number average molecular weights (M_n), its distributions (M_w/M_n), and the ratio of *cis* carbon-carbon double bonds are listed in Table 1. Poly(**Y**) was obtained in EtOH in 95% yield, and poly(**R**) was obtained in Hex in 84% yield, respectively. Their *cis*%s were carefully calculated based on the integration ratio of vinyl proton and methyl or methylene protons observed in the ^{1}H NMR spectra.[26,27] Previously, we have reported that an organic solvent such as EtOH or NEt_3 with lone pair electrons induces the dissociation of the dimeric Rh complex catalyst to give a substantial monomeric species, which is stabilized with the solvent and causes a good polymerization.[18a,c,26] In contract, Hex has not been used as the polymerization solvent, and its solvent effect has not been known, up to date to the best of our knowledge.

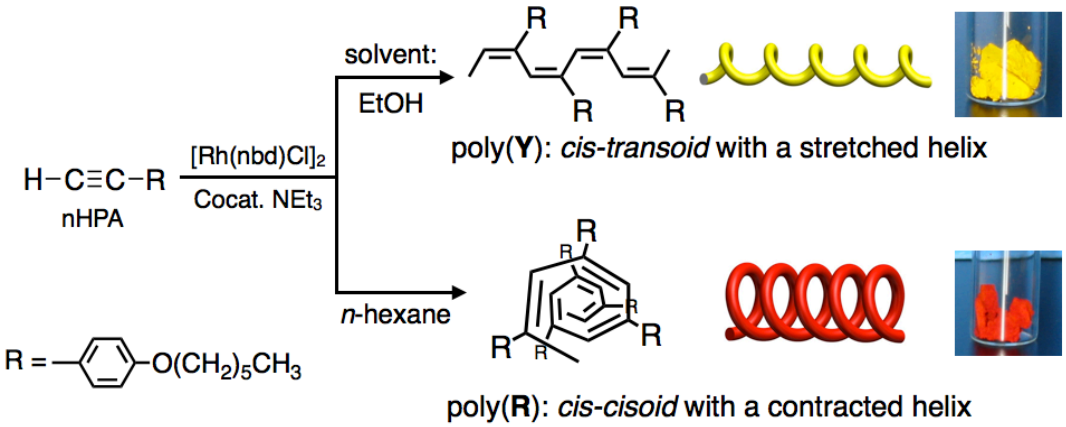

Scheme 1. Synthesis of poly(*p*-*n*-hexyloxyphenylacetylene)s having a stretched *cis-transoid* helix and a contracted *cis-cisoid* helix using a $[Rh(nbd)Cl]_2$-NEt_3 catalyst in ethanol or *n*-hexane.

Table 1. Polymerization of pHPA with a $[Rh(nbd)Cl]_2$- NEt_3 Catalyst.[a]

polymer	solvent[b]	yield[d] (%)	M_n[e] x10^{-4}	M_w/M_n[e]	*cis*[f] (%)	color	λ_{max}[g] (nm)	d_{obs}[h] (Å)
poly(**Y**)	EtOH	95	8.5	2.6	91	bright yellow	445	24.9
poly(**R**)	*n*-hexane	84	5.3	2.3	92	purple red	575	30.0
poly(**Y**→**B**)	-[c]	-	4.2	2.7	91	reddish black	570	29.3

[a] Polymerization conditions: 25 °C, 0.5 h, $[M]_0$ = 0.20 M, $[M]_0/[Rh\ cat.]$ = 100, $[NEt_3]/[Rh\ cat.]$ = 100. [b] Polymerization solvent used. [c] Prepared by thermal treatment of poly(**Y**) at 80 °C for 1 h under N_2. [d] MeOH insoluble part. [e] Estimated by GPC analysis (PSt, $CHCl_3$). [f] Determined by ^1H NMR analysis ($CDCl_3$). [g] Measured by DRUV-Vis method. [h] Diameters of columnar determined by XRD analysis.

Solid Phase DRUV-Vis Spectra

The DRUV-Vis spectra of poly(**Y**) and poly(**R**) were shown in Figure 1. The absorption maximum, λ_{max}, of poly(**Y**) was observed at 445 nm, which was notably shorter compared to 575 nm of poly(**R**). A similar color change has not been reported for PnHPAs. It has been reported that poly(phenylacetylene) (PPA) prepared in a $Fe(acac)_3$-$AlH(i\text{-}Bu)_2$ catalytic system was a red insoluble polymer,[1] and poly(*p*-methylphenylacetylene) (PMPA) prepared with the Rh complex catalyst was a red solid powder which was insoluble to ordinary organic solvents.[24] The spectrum of poly(**R**) appears to hide an absorption peak in a shoulder around at 360−445 nm in an addition to a peak at 575 nm, suggesting that poly(**R**) is composed from two kinds of conjugated systems. On the other hand, λ_{max} of poly(**Y**) was observed at 445 nm in a fairly narrower absorption peak compared to that of poly(**R**). Previously *cis* and *trans* polyacetylenes with no substituent prepared by the Ziegler-Natta catalyst, Et_3Al-$Ti(On\text{-}Bu)_4$, have been reported to show two λ_{max}s at 570 nm and 675 nm, respectively.[25] It seems that the λ_{max} of poly(**R**) is quite similar to that of the so-called Shirakawa polyacetylene with *cis* conjugation sequences.[25]

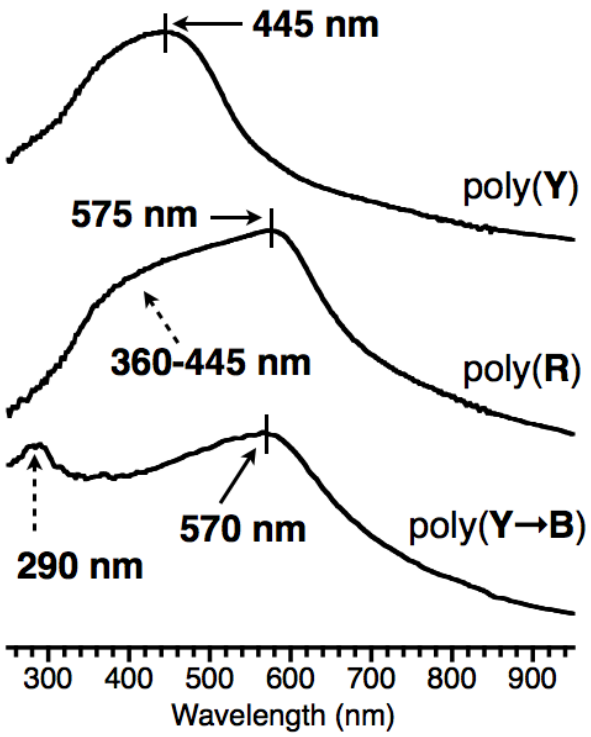

Figure 1. DRUV–vis spectra of poly(**Y**), poly(**R**), and poly(**Y**→**B**) observed on alumina powder.

The solution UV spectra of poly(**Y**) and poly(**R**) measured in chloroform at room temperature showed similar absorption maxima at 290, 340, and 410 nms without a significant difference, as shown in Figure 2. Their absorptions may be assigned to the absorptions due to the monomer unit moiety involving one *cis* C=C, relatively short helical sequences, and/or helical main-chain conjugation comprising a few monomer unit moieties. These UV-vis spectra seems that at least the color difference is not related to the degree of the polymer concentration difference between poly(**Y**) and poly(**R**) because the same concentration solutions were used. Alternatively, the difference of polymer color in solid phase may be ascribable to that of morphology

and/or helical structures as mentioned below.

Figure 3 shows the resonance laser Raman spectra of poly(**Y**) and poly(**R**) measured in solid phase using an Ar^+ laser using samples obtained after mixing 3 mg of each polymer and 200 mg of KBr with a mortar and pestle. The absorption bands at 1530, 1335, and 965 cm^{-1} were assigned to those of *cis* C=C bond and/or phenyl ring, *cis* C-C bond and/or C-C bond between the main-chain and phenyl ring, and *cis* C-H bond, respectively, as reported before.[22,26]

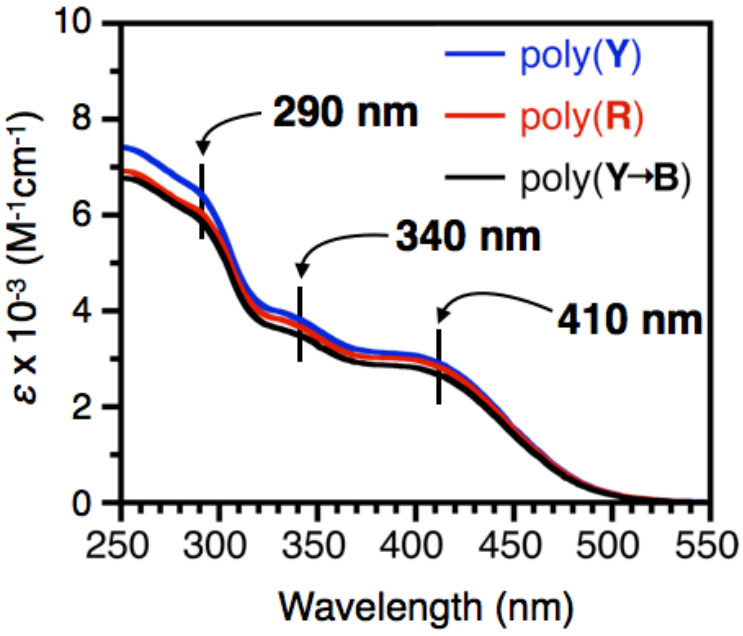

Figure 2. Solution UV–vis spectra of poly(Y), poly(R), and poly(Y→B) observed in chloroform at room temperature.

We found that there are fairly large differences, especially in the peak corresponding to the *cis* C=C bond over-rapped with the phenyl ring at around 1530 cm^{-1} between

them. The Raman spectrum of poly(**Y**) appeared in fairly broader band compared to that of poly(**R**).

The broad peak suggests that poly(**Y**) takes rather disordered and/or disturbed structures in thermodynamically more unstable form compared to that of poly(**R**). It is also noteworthy that the peaks due to *trans* C=C bond, e.g., 1500 cm^{-1} and 1210 cm^{-1} were never observed in the present polymers,[23,27] though the *trans* ratio for poly(**R**) and for poly(**Y**) were estimated to be 8% and 9%, respectively, using ^{1}H NMR spectra of them. It is noteworthy that their Raman spectra of poly(**R**) and poly(**Y**) together with their DRUV-Vis spectra observed in solid phase have never been reported up to date to the best of our knowledge.

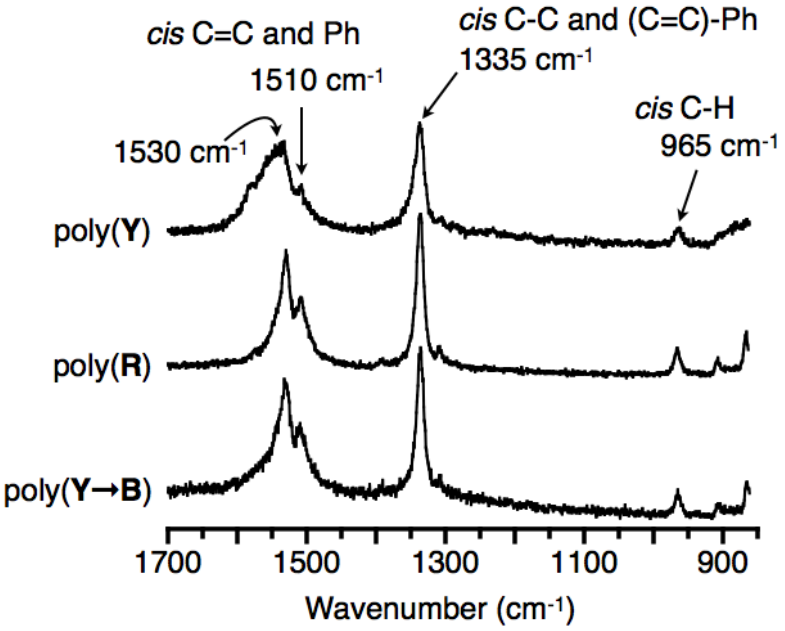

Figure 3. Laser Raman spectra of poly(Y), poly(R), and poly(Y→B) observed on KBr powder.

^{1}H NMR Spectra

As shown in Figure 4, the ^{1}H NMR spectra of poly(**Y**) and poly(**R**) were measured in $CDCl_3$ solution at room temperature. In both spectra, the peaks observed at 6.60 and 6.43, 5.75, 3.67, 1.66, 1.39-1.13, and 0.89 ppm were assigned to those of phenyl, H-C=C, OCH_2, OCH_2CH_2, $(CH_2)_3$, and CH_3, respectively. There are basically no large difference in chemical shift, line shape and line width, irrespective of notably large color difference between them in solid phase, though the ^{1}H NMR spectrum of poly(**R**) is not shown. This suggests that the color of the solid polymers is never distinguished in the solution, though the color of the both polymers never faded even in EtOH. Therefore, the origin of the color difference may be ascribed to the morphological and/or conformational difference. In other words, to explain difference in color between poly(**Y**) and poly(**R**), an existence of some stretched and contracted pitch polymers corresponding to *cis-transoid* and *cis-cisoid* helices may be considered, though the structural differences are unable to be detected in the solution.[18(a,c)]

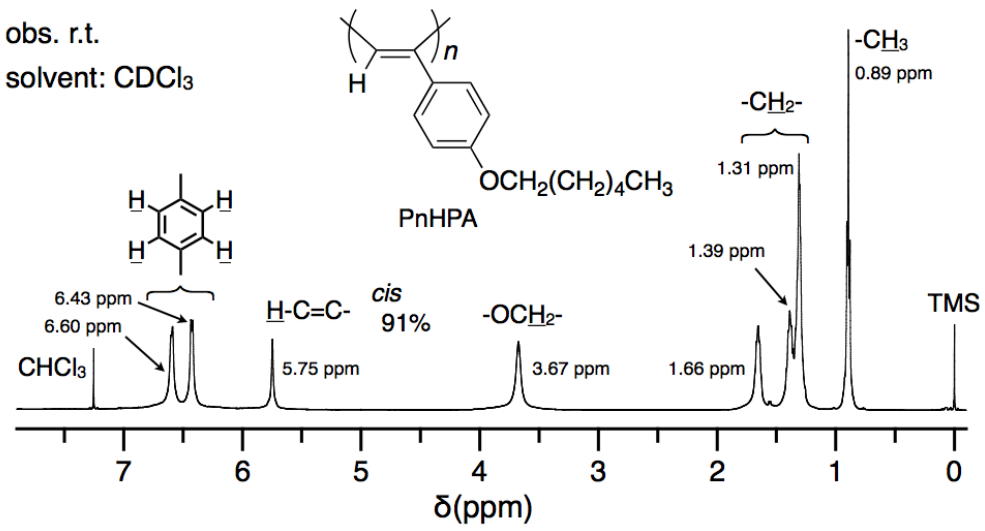

Figure 4. ^{1}H NMR spectra of poly(**Y**) observed in $CDCl_3$ solution.

Because the exchange speed between them may be too fast to be differentiated each other judging from the time scale of the present ^{1}H NMR spectrometer at room temperature.

X-ray Diffraction

Figures 5 and 6 show the XRD patterns of poly(**Y**) and poly(**R**) measured in the temperature range form 30 °C to 140 °C in air. From the pattern denoted with a dotted line measured at 30 °C the formation of psuedohexagonal crystal called a columnar is deduced and its crystal is composed from a polymer assemble due to the helical *cis-transoid* main-chain.[7d,15,24,27] The reflection peaks at 2θ = 4.2° and 20° were assigned to those of the (100) and amorphous halo superposed with an intramolecular hexyloxy chain distance as the side chain of poly(**Y**), as reported before.[27]

Furthermore, the diameter of poly(**Y**) having the helical *cis-transoid* structure was determined to be 24.9 Å. The XRD pattern of poly(**R**) having the helical *cis-cisoid* main-chain was also analyzed. The formation of a similar columnar was assumed, and the diameter of poly(**R**) was determined to be 30.0 Å. The diameter of poly(**Y**) is thus found to be smaller by 5.1 Å than that of poly(**R**). Further a fairly small peak was observed at around $2\theta = 26°$, i.e., d = 3.4 Å in each polymer whose intensity is much lower in poly(**Y**) compared to that of poly(**R**), as shown in Figures 5 and 6. This fact suggests that the intramolecular distance between the neighbouring benzene rings and/or C=C bonds is 3.4 Å, and this fairly narrow distance is approximately the same as that of a typical layer compound such as graphite.[28] This implies that an intramolecular π-conjugation, that is, the so-called π-stacking takes place between the neighbor phenyl rings and/or the *cis* C=C bonds each other along to the axis of the helical polymer chains and the degree of the π-stacking conjugation in poly(**R**) is much stronger than that of poly(**Y**). Consequently, it is said that the stronger π-stacking created in poly(**R**) caused the larger red-shift of poly(**R**) compared to that of poly(**Y**) in their solid phase UV spectra.

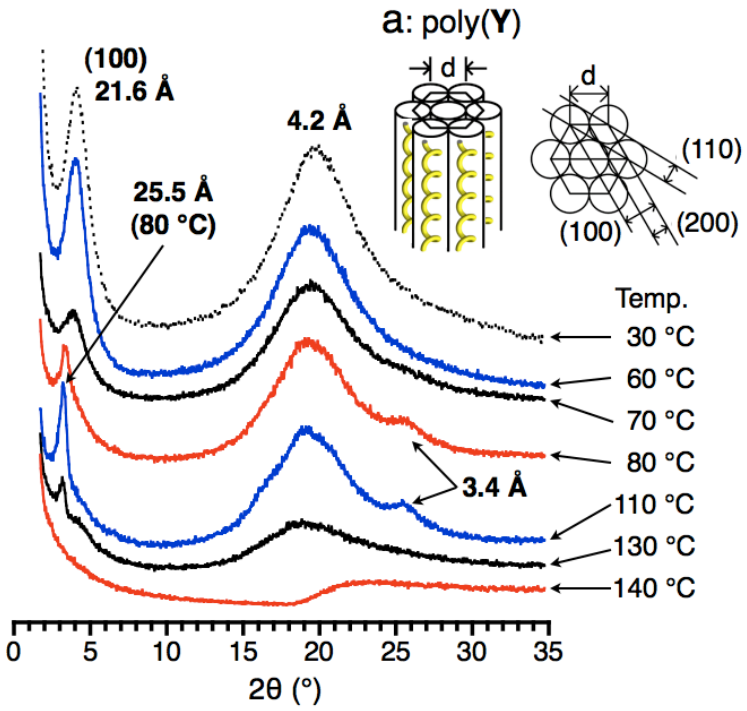

Figure 5. Temperature dependences of the XRD patterns of poly(Y).

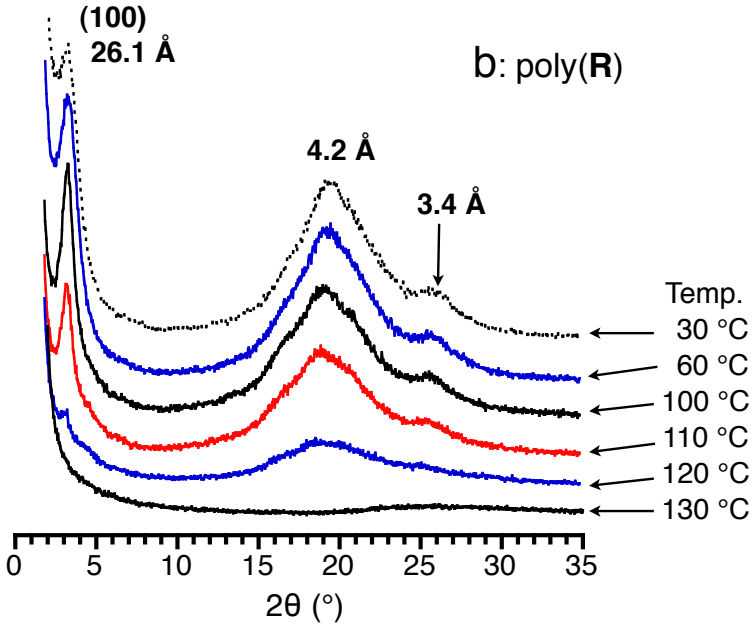

Figure 6. Temperature dependences of the XRD patterns of poly(R).

Thermally Induced Helical Rearrangement from Cis-transoid to Cis-cisoid

We found that the reflection peak intensity of poly(**Y**) was decreased with increasing the observed temperature, as shown in Figure 5. Especially the speed of decreasing intensity was fairly rapid at 70−80 °C, as shown in Figure 5. Furthermore, a new peak was gradually created at 2θ = 3.4°, Bragg distance d = 25.5 Å as a new (100) reflection, and decayed completely at around 140 °C. These pattern changes may correspond to the so-called *cis*-to-*trans* isomerization,[9a,18a,19] and be explained in terms of the phase transition to thermodynamically more stable form, such as from the *cis-transoid* helix to *cis-cisoid* helix. This thought is strongly supported by the fact that the newly appeared peak at d = 25.5 Å is approximately comparable to that of the diameter, 26.1 Å of poly(**R**) having a *cis-cisoid* helix, which is composed from a fairly narrow contracted pitch, i.e., 3.4 Å as mentioned above. This distance corresponds to that of a typical layer compound such as graphite where the p-stacking takes place along the molecular axis which is correlated to the electrical conductivity.[28] However, we could not find the reverse thermally induced pattern change of poly(**R**), and the reflection intensity was simply decreased with increasing the temperature, as shown in Figure 6. This also supports that poly(**R**) in solid phase is thermodynamically more stable helix compared to that of poly(**Y**), Therefore, based on these XRD pattern changes it is concluded that poly(**Y**) having a helical *cis-transoid* pitch can rearrange to the thermodynamically more stable poly(**R**) having a narrower helical pitch in the *cis-cisoid* helix. The thermally rearranged polymer, poly(**Y→B**), showed a reddish black color (Scheme 2). The DRUV-Vis absorption maximum observed after the heat-treatment of poly(**Y**) is

almost coincided to that, 575 nm of the pristine poly(**R**), though a small peak was newly generated at around 290 nm as shown in Figure 1.

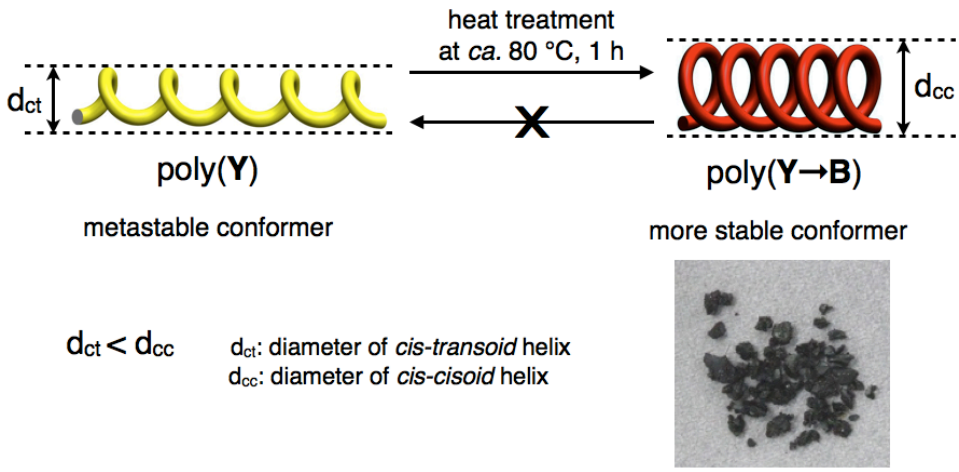

Scheme 2. Structural rearrangement from poly(Y) to poly(Y → B) induced by heat-treatment at 80 ℃ for 1 h accompanied with a color change.

Molecular Mechanics Calculation

The energetically most stable conformations of both poly(**Y**) and poly(**R**) were simulated using 20-mer of pHPA as a model polymer molecule by a molecular mechanics (MM) calculation using a MMFF94 force field,[21] as shown in Figure 7. The MMFF94 calculation undoubtedly revealed that the energetically favored polymer structures for poly(**Y**) and poly(**R**) have a stretched *cis-transoid* helix with its columnar diameter of 24.7 Å and the contacted *cis-cisoid* helix with its columnar diameter of 29.1 Å, respectively.

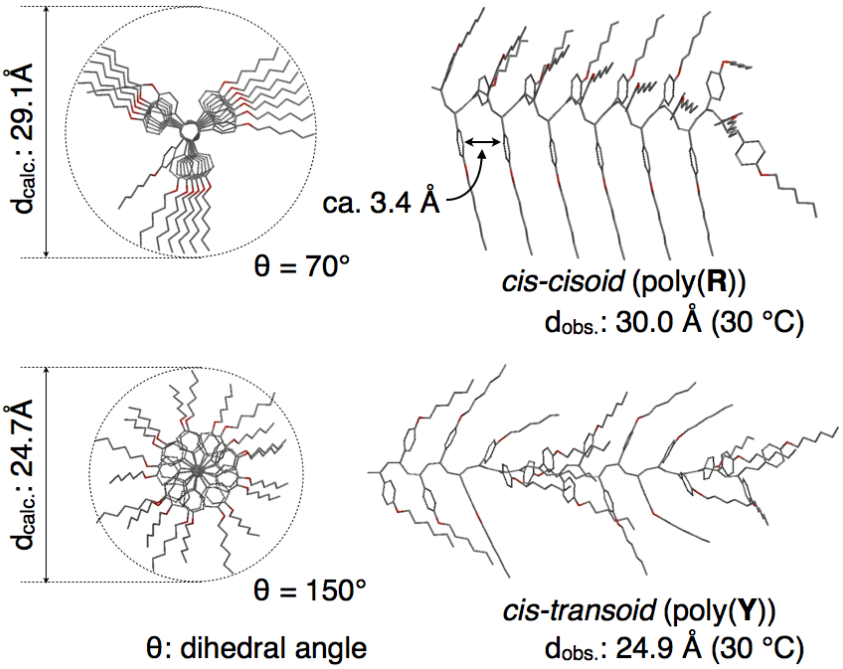

Figure 7. Cis-transoid and cis-cisiod helices and dihedral angles, θ°, calculated by MMFF94 force field.

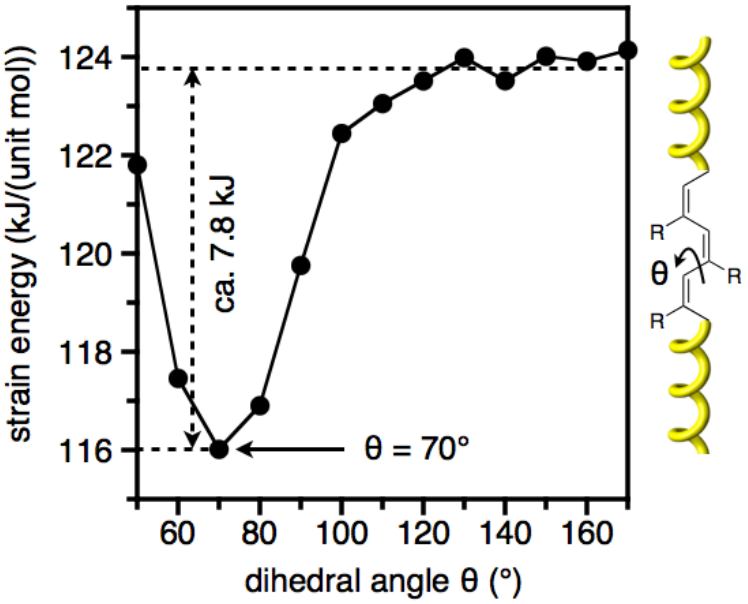

Figure 8. Strain energy dependences of dihedral angle around C-C single bond in the C-C-C=C sequence in the main chain.

Thus, the observed and calculated diameters are well agreed each other within 0.2-0.9 Å, indicating a reliability of our analysis. It shows that the thermal treatment of poly(**Y**) at 80 ℃ expanded its helix diameter by ~ 3.8 Å, which value was observed in the XRD pattern (Fig. 5). Figure 8 shows a relation between the dihedral angle θ° connecting two C=C bonds in the *cis-transoid* configuration making a C=C-C=C bond in the main-chain and strain energy (kJ/(unit mol)). This result clearly shows that the strain energy of the dihedral angle becomes minimum at 70° which is also substantially agreed to that of the angle, about 70° calculated by the XRD studies. The layer distance corresponding to the helical pitch in 20-mer used as the model of poly(**R**) was also calculated to be 3.4 Å. This indicates that the observed layer distance can be exactly reproduced through the MM calculation.

Column Diameters

The temperature dependence of the columnar diameters of poly(**Y**) and poly(**R**) at the temperature from 30 °C to 130 °C under N_2 was observed by the XRD method, as shown in Figure 9. The diameter of poly(**Y**) was notably changed from 24.9 Å to 29.3 Å at 80 °C, but poly(**R**) did not. This clearly indicates that the thermal rearrangement took place leading to the structure isomerization from the stretched *cis-transoid* helix to the contracted *cis-cisoid* helix.

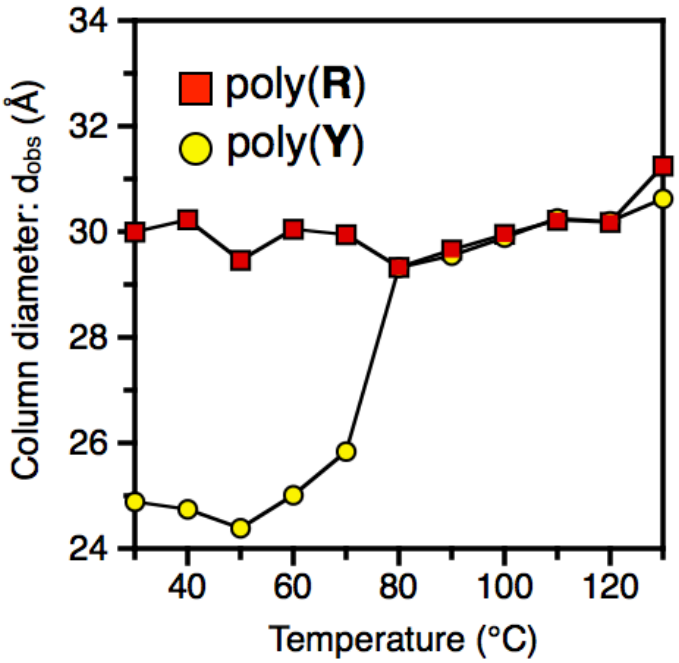

Figure 9. Temperature dependences of the columnar diameters of poly(**Y**) and poly(**R**) measured by XRD method.

DSC Studies

Figure 10 shows the DSC traces of poly(Y) and poly(R) measured at the heating rate of 1 or 10 °C/min. in the temperature range from 30 °C to 200 °C in an atmosphere of nitrogen. Poly(Y) showed two exothermic peaks at *ca*. 80 °C and 140 °C, respectively, which correspond to the rearrangement temperatures from the *cis-transoid* helix to the *cis-cisoid* helix and the thermal *cis*-to-*trans* isomerization, as mentioned above.

It is essentially noteworthy that the thermal treatment of poly(Y) at 80 °C for 1 h under N_2 atmosphere did not decrease the *cis*% because the *cis*-to-*trans* isomerization temperature is much higher, i.e., approximately 130 °C than that of the thermal treatment temperature. No such an exothermic peak in poly(R) was observed except for

an isomerization peak at around 140 °C and melting points due to a *n*-hexyloxy side chain which is shown in both polymers were observed at 61−67 °C when the heating rate was increased from 1 to 10 °C/min., as shown in Figure 10b. The enthalpy of transition, *DH*(kJ/(unit mol), corresponding to the thermally induced rearrangement of poly(Y) to poly(Y→B) was estimated to be 1.6 kJ/(unit mol), which is approximately 1/5 of the calculated value, 7.8 kJ/(unit mol) obtained by the MMFF94 method as shown in Figure 8. This inconsistency may be explained in terms of the columnar structure of poly(Y) which is assemble of the *cis-transoid* helix main-chain. A fairly large energy may be necessary to generate the *cis-cisoid* helix polymer, poly(Y→B) from poly(Y) in solid phase because the columnar of *cis-cisoid* helix polymer is newly reconstructed. Therefore, the thermally induced rearrangement may not proceed smoothly or quantitatively, in other words, at least around less than 1/2 of the helix component in poly(Y) may only rearrange to the *cis-cisoid* helix jugging from the DRUV-Vis spectra (see Figure 1). This also suggests that a half of poly(Y) remains unchanged as it is when poly(Y) was heated even at 80 °C. Consequently the boundary sequences between the unchanged poly(Y) and the changed poly(Y→B) which is a relatively short and distorted sequences and show a small absorption at around 290 nm as shown in Figure 1. Thus, this inconsistency is reasonably explained if the solid phase structural rearrangement between the *cis-transoid* helix and *cis-cisoid* helix is not proceeded easily.

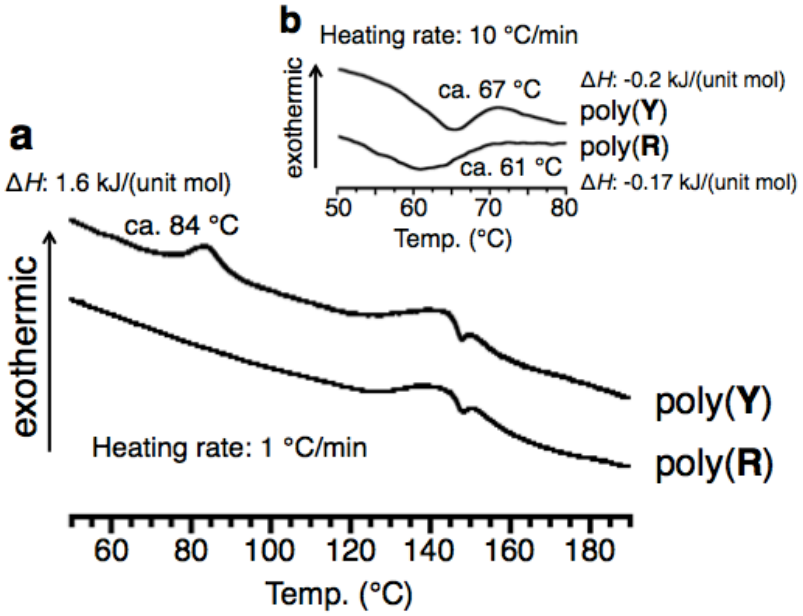

Figure 10. DSC traces of poly(**Y**) and poly(**R**) observed under N_2 atmosphere.

Conclusion

The stereospecific polymerization of *p*-*n*-hexyloxyphenyacetylene, *p*HPA, was successfully performed using a Rh catalyst, $[Rh(nbd)Cl]_2$-NEt_3 in EtOH or Hex at 25 °C to afford poly(**Y**) with a bright yellow color and poly(**R**) with a purple red color as powders selectively in fairly high yields. The structures and colors of the polymers were investigated not only in solution but also in solid phase using ^{1}H NMR, DRUV-Vis, UV-Vis, and resonance Raman spectra, XRD, and MM calculation, together with DSC method. Poly(**Y**) and poly(**R**) showed an absorption maximum, λ_{max}, at 445 nm or 575 nm in solid phase, respectively. In chloroform, no significant difference was observed between the both polymers. The line width of Raman spectrum for poly(**Y**) was wider than that of poly(**R**). This suggested that the polymer structure of poly(**Y**) is a more

disordered than that of poly(**R**). The former is therefore considered to be thermodynamically less stable.

The XRD patterns suggested columnar structures comprising of the helical chains for both polymers, and their diameters were found to be 24.9 Å for poly(**Y**) and 30.0 Å for poly(**R**), respectively. A small peak at d = *ca*. 3.4 Å was assigned to the layer distant, which was corresponding to an average helical pitch. The pitch of poly(**R**) is narrower than that of poly(**Y**). Interestingly a thermally induced rearrangement of the yellow poly(**Y**) to a reddish black polymer, poly(**Y→B**) took place at 80 °C. Such structural and helical changes associated with a drastic color change have never been reported before to the best our knowledge. Poly(**Y→B**) showed a λ_{max} at 570 nm accompanying with a very wide absorption peak from 300 nm to 900 nm which may give a dark red color in this polymer. The observed helix diameter, 30.0 Å in columnar of poly(**R**) is near to that, 29.3 Å of the diameter of poly(**Y→B**) (Figures 5 and 6). This means that poly(**Y**) is thermodynamically less stable helix compared to that of poly(**R**). The thermal instability of poly(**Y**) was proven by the fact that its exothermic transition temperature was observed at 80 °C. Thus, these data clearly indicate that the stretched helix polymer, poly(**Y**), was changed to the contracted helix polymer, poly(**Y→B**), when heated at 80 °C under N_2.

Reference

1. R. J. Kern, *J. Polym. Sci., Polym. Chem. Ed.* **1969**, 7, 621-631.

2. L. B. Luttinger, *J. Org. Chem.* **1962**, 27, 1591-1596.

3. F. D. Kleist, N. R. Byrd, *J. Polym. Sci: Polym. Chem. Ed.* **1969**, 7, 3419.

4. P. Biev, A. Furlani, M. V. Russo, *Gazz. Chim. Ital.* **1980**, 110, 25.

5. A. Furlani, P. Biev, M. V. Russo, A. Fiorentio, *Gazz. Chim. Ital.* **1987**, 117, 373.

6. T. Masuda, T. Higashimura, *Adv. Polym. Sci.* **1986**, 81, 121-165.

7. (a) M. Tabata, W. Yang, K. Yokota, *Polym. J.* **1990**, 22, 1105-1107. (b) W. Yang, M. Tabata, K. Yokota, *Polym. J.* **1991**, 23, 1135-1138. (c) M. Tabata, W. Yang, K. Yokota, *J. Polym. Sci. Part A: Polym. Chem.* **1994**, 32, 1113-1120. (d) Y. Yoshida, Y. Mawatari, C. Seki, T. Hiraoki, H. Matsuyama, M. Tabata, *Polymer* **2011**, 52, 646-651.

8. (a) Y. Kishimoto, P. Eckerle, T. Miyataka, M. Kainosho, A. Ono, T. Ikariya, R. Noyori, *J. Am. Chem. Soc.* **1999**, 121, 12035-12044. (b) N. Onishi, M. Shiotsuki, F. Sanda, T. Masuda, *Macromolecules* **2009**, 42, 4071-4076. (c) T. Nishimura, Y. Ichikawa, T. Hayashi, N. Onishi, M. Shiotsuki, T. Masuda, *Organometallics* **2009**, 28, 4890-4893. (d) M. Shiotsuki, N. Onishi, F. Sanda, T. Masuda, *Chem. Lett.* **2010**, 244-245. (e) M. Shiotsuki, F. Sanda, T. Masuda, *Polym. Chem.* **2011**, 2, 1044-1058.

9. (a) T. Sone, R. Amato, Y. Mawatari, M. Tabata, A. Furlanl, M. V. Russo, *J. Polym. Sci. Part. A: Polym. Chem.* **2004**, 42, 2365-2376. (b) H. Nakako, R. Nomura, M. Tabata, T. Masuda, *Macromolecules* **1999**, 32, 2861-2864.

10. T. Masuda, E. Isobe, T. Higashimura, K. Takada, *J. Am. Chem. Soc.* **1983**, 105, 7473-7474.

11. (a) T. A. Skotheim, Ed. Handbook of Conducting Polymers; Dekker: New York, **1986**, vol. 1-2. (b) J. R.Ferraro, J. M. Williams, Eds. Introduction to Synthetic

Electrical Conductors; Acad. Press Inc: New York **1987**. (c) J. C. Salomone, Ed. Polymeric Materials; CRC Press: New York **1996**, vol. 8, 6481.

12. (a) A. Asdente, A. Ottoboni, A. Furlani, M. V. Russo, Chemtronics **1991**, 5, 75-80. (b) A. Furlani, G. Iucci, M. V. Russo, A. Bearzotti, R. D'Amico, Sens Actuators B **1992**, B7, 447-450.
13. (a) D. Neher, A. Wolf, C. Bubeck, G. Wegner, *Chem. Phys. Lett.* **1989**, 163, 116-122. (b) J. L. Bredas, C. Adant, P. Tacks, A. Persoons, M. Pierce, *Chem. Rev.* **1994**, 94, 243-278. (c) M. Falconieri, R. D'Amato, M. V. Russo, A. Furlani, *Nonlinear Opt.* **2001**, 27, 439-442. (c) M. Tabata, T. Sone, K. Yokota, T. Wada, H. Sasabe, *Nonlinear Opt.* **1999**, 22, 341-344. (d) T. Wada, L. Wang, H. Okawa, T. Masuda, M. Tabata, M. Wan, M. Kakimoto, Y. Imai, H. Sasabe, *Mol. Cryst. Liq. Cryst.* **1997**, 294, 245-250.
14. (a) T. Aoki, K. Shinohara, E. Oikawa, *Chem. Lett.* **1993**, 22, 2009-2012. (b) M. Teraguchi, J. Suzuki, T. Kaneko, T. Aoki, T. Masuda, *Macromolecules* **2003**, 36, 9694-9697. (c) Y. Suzuki, J. Tabei, M. Shiotsuki, Y. Inai, F. Sanda, T. Masuda, *Macromolecules* **2008**, 41, 1086-1093. (d) E. Yashima, Y. Maeda, Y. Okamoto, *J. Am. Chem. Soc.* **1998**, 120, 8895-8896. (e) E. Yashima, T. Matsushima, Y. Okamoto, *J. Am. Chem. Soc.* **1997**, 119, 6345-6359. (f) R. Nonokawa, E. Yashima, *J. Am. Chem. Soc.* **2003**, 125, 1278-1283.
15. Y. Mawatari, M. Tabata, *J. Jpn. Soc. Colour Mater* **2009**, 82, 204-209.
16. (a) Y. V. Korshak, T. V. Medvedeva, A. A. Ovchinnikov, V. Spector, *Nature* **1987**, 326, 370-372. (b) N. Tyutyulkov, K. Müllen, M. Baumgarten, A. Ivanova, A. Tadjer,

Synth. Met. **2003**, 139, 99-107. (c) M. Tabata, Y. Nozaki, W. Yang, K. Yokota, Y. Tazuke, *Proc. Jpn. Acad.* **1995**, 71, 219-224. (d) K. H. Fisher, J. A. Herz, Spin glass; Cambridge University Press: **1991**, 30. (e) J. J. Pregjean, J. Souletie, *J. Phys.* **1980**, 41, 1335-1352. (f) L. Floch, F. Hammann, J, Ocio, M. Vincent, *Euro. Phys. Lett.* **1992**, 18, 647-652. (g) D. G. Xenikos, H. Multer, C. Jouan, A. Suilpice, J. L. Tholence, *Solid. State. Commun.* **1997**, 102, 681-685. (h) M. Tabata, Y. Watanabe, S. Muto, *Macromol. Chem. Phys.* **2004**, 205, 1174-1178. (i) Y. Watanabe, S. Muto, M. Tabata, *Jpn. J. Appl. Phys. Part 2 Lett.* **2004**, 43, 300-302.

17. M. Kozuka, T. Sone, M. Tabata, Y. Sadahiro, T. Enoto, *Radiation Phys. Chem.* **2002**, 63, 59-61.
18. (a) C. I. Shimionescu, V. Percec, S. Dumitrescu, *J. Polym. Sci: Polym. Chem. Ed.* **1977**, 2497-2509. (b) M. Tabata, Y. Inaba, K. Yokota, Y. Nozaki, *J. Macromol. Sci. Pure Appl. Chem.* **1994**, A31, 465-475. (c) V. Percec, G. J. Rudick, M. Peterca, M. Wagnar, M. Obata, M. C. Mitchell, W. Cho, S. K. V. Balagurusamy, A. P. Heiney, *J. Am. Chem. Soc.* **2005**, 127, 15257-15264.
19. R. D'Amato, T. Sone, M. Tabata, Y. Sadahiro, M. V. Russo, A. Furlani, *Macromolecules* **1998**, 31, 8660-8665.
20. K. Weiss, G. Beernink, F. Dötz, A. Berliner, K. Müllen, G. H. Wöll, *Angew. Chem. Int. Ed.* **1999**, 38, 3748-3752.
21. MMFF94 calculations were carried out with Spartan'04 Windows ver. 1.03 (Wavefunction, Inc.).
22. A. Miyasaka, T. Sone, Y. Mawatari, S. Setayesh, K. Müllen, M. Tabata, *Macromol.*

Chem. Phys. **2006**, 207, 1938-1944.

23. M. Tabata, T. Sone, Y. Sadahiro, K. Yokota, *Macromol. Chem. Phys.* **1998**, 199, 1161-1166.
24. M. Tabata, S. Kobayashi, Y. Sadahiro, Y. Nozaki, K. Yokota, W. J. Yang, *Macromol. Sci. Pure. Appl. Chem.* **1997**, A34, 641-653.
25. (a) H. Shirakawa, T. Ito, S. Ikeda, *Macromol. Chem.* **1978**, 179, 1565-1573. (b) T. Harada, M. Tasumi, H. Shirakawa, *Chem. Lett.* **1978**, 1411.
26. M. Tabata, T. Sone, Y. Sadahiro, *Macromol. Chem. Phys.* **1999**, 200, 265–282.
27. Y. Mawatari, M. Tabata, T. Sone, K. Ito, Y. Sadahiro, *Macromolecules* **2001**, 34, 3776-3782.s
28. I. L. Spain, The Physics of Semimetals and Narrow Band-Gap Semiconductors; Carter, D. L.; Bate, R. T. Eds.; Pergamon Press: Oxford, **1971**, p 117.

Chapter 2

Contracted Helix to *Stretched Helix* Rearrangement of an Aromatic Polyacetylene Prepared in *n*-Hexane with [Rh(norbornadiene)Cl]$_2$-triethylamine Catalyst

Abstract

p-*n*-Heptylphenylacetylene (*p*HepPA) was stereoregularly polymerized in *n*-hexane at 25 °C using $[Rh(nbd)Cl]_2$ catalyst and NEt_3, affording the purple-red Poly(**R**) in 97 % yield. A 80 °C heat treatment transformed Poly(**R**) to the black Poly(**B**). The Poly(**R**) XRD pattern revealed a hexagonal crystal structure comprising ***contracted*** *cis-cisoid helices* (^{Hexa}Poly(**R**)^{CC}). The 80 °C heat treatment generated two tetragonal crystals: ^{Tetra}Poly(**B**)^{CC} containing ***contracted*** *cis-cisoid helices* and ^{Tetra}Poly(**B**)^{CT} containing ***stretched*** *cis-transoid* helices. The helical diameters before and after heat treatment were estimated using XRD and were consistent with MMFF 94 calculations. When heated at 80 °C in the solid phase, the λ_{max} in the diffuse reflective UV-vis spectra of ^{Hexa}Poly(**R**)^{CC} shifted from 482 nm to 560 nm. Additionally, an endothermic transition occurred in the ^{Hexa}Poly(**R**)^{CC} DSC trace at approximately 80 °C. Therefore, these data corroborated the assertion that ^{Hexa}Poly(**R**)^{CC} thermally converted to ^{Tetra}Poly(**B**)^{CC} and ^{Tetra}Poly(**B**)^{CT}.

Introduction

During the past two decades, bidentate rhodium complexes, e.g., $[Rh(nbd)Cl]_2$-cocatalysts (nbd: norbornadiene),[1] zwitterionic Rh complexes,[2] and cationic $Rh^+BF_3^-$ complexes,[3] have become important stereoselective polymerization catalysts for the creation of *helical* substituted polyacetylenes (SPAs) with *cis-transoid* geometrical structures from various substituted acetylene (SA) monomers. A monodentate Rh complex has been reported as the active catalyst, and this species is generated *in situ* when triethylamine (TEA), alcohols, or aqueous alcohols are used as cocatalyst or solvent.[4] SPAs having *helical cis-transoid* structures are associated with chiroptical properties[5,6] and are driven by van der Waals forces to produce columns of pseudohexagonal crystals in the solid state.[7] The *helical* pitch of an alkoxy-substituted poly(phenylacetylene) can be controlled using external stimuli. For example, thermal treatment of the solids or exposure to solvent vapor converts the ***stretched*** *cis-transoid* ***helices*** to ***contracted*** *cis-cisoid* ***helices***, and this transformation is accompanied by a drastic color change from bright yellow to dark red.[8] However, the morphology of these polymers and the mechanism of their solid phase transformations have not been thoroughly investigated despite the polymers' many interesting physicochemical properties: oxygen permeability,[9] nonlinear optical behavior,[10] electrical conductivity,[11] time and temperature memory effects,[12] enantioselectivity, and responsiveness to external stimuli.[13]

Recently, the chiral-side-chain-induced formation of predominantly one-handed SPA *helices* was explained by CD spectral data, and CD spectral data were also used to

explain their dynamical *helix* inversions.[14,5] PPAs prepared using Ziegler-Natta[15] and metathesis catalysts[16] have interfered with the polymers' own geometrical and spatial structure analysis by ^{1}H and ^{13}C NMR. These interferences occurred because gels, large quantities of irregular sequences, e.g., *head*-to-*head* or *tail*-to-*tail* bond units, or unpaired electrons were present in the polymers. The unpaired electrons were generated through the rotational scission of *cis* C=C bonds by thermal *cis*-to-*trans* isomerization,[17] compression,[8(b)] and the polymerization itself.[17(c),18]

In Chapter 1, we found that *p*-*n*-hexyloxyphenyacetylene afforded poly(**Y**) with a bright yellow color and poly(**R**) with a purple red color which are dependent on different of polymerization solvent used. In this report, we changed the structure of monomer from *p*-*n*-hexyloxyphenyacetylene to *p*-*n*-heptylphenylacetylene in order to determine whether the helical pitch can be controlled.

In this report, *p*-*n*-heptylphenylacetylene (*p*HepPA) was polymerized in *n*-hexane at room temperature using a Rh-complex catalyst and TEA cocatalyst, affording the purple-red poly(*p*HepPA) (Poly(**R**)) with a ***contracted*** *cis-cisoid helical* structure. Moreover, we report a solid state *helix* rearrangement from ***contracted*** to ***stretched*** that was induced by heating from 30 °C to 80 °C, in contrast with the previous case. To the best of our knowledge, such an irreversible rearrangement of crystal form associated with the color change has not been reported,[19] although the static and dynamical behaviors of these *helices* are significant features of these p-conjugated polymers.[20] Furthermore, determining whether the ***contracted*** *cis-cisoid* ***helix*** (***contracted helix***^{CC}) is generated as a stable structure is important. The SPA ***contracted helix***^{CC} was

considered a missing *helix* for a long time and was only recently identified in solution[21] and solid phases.[8(a)] Recently, we reported that the ***helical*** backbones of *achiral* and *chiral* aliphatic polyacetylene esters exhibit an interesting "***accordion-like oscillation*** of the ***helical (HELIOS)*** main chain" in solution. Morphology before and after the Poly(**R**) thermal treatment was evaluated using ^{1}H and ^{13}C NMR spectroscopy, wide-angle X-ray diffraction (XRD), differential scanning calorimetry (DSC), solid phase UV-vis spectroscopy, and molecular mechanics calculations (MMFF94 force field method).

Experimental Section

Materials

MeOH, *n*-hexane (*n*Hex), and triethylamine (TEA) (JUNSEI Chemical Co.) were distilled before use. $[Rh(nbd)Cl]_2$ (nbd = norbornadiene) was purchased from Aldrich and used without further purification.

Monomer Synthesis

The monomer, *p*-*n*-heptylphenylacetylene (*p*HepPA) was prepared according to a literature procedure[22] and purified by silica gel column chromatography using *n*-hexane as eluent. ^{1}H NMR (500 MHz, $CDCl_3$, ppm): 7.40 (Ph-*H*, d, *J* = 8.3 Hz, 2H), 7.12 (Ph-*H*, d, *J* = 8.0 Hz, 2H), 3.02 (C≡C*H*, s, 1H), 2.59 (Ph-CH_2, t, *J* = 15.5 Hz, 2H), 1.61-1.57 (CH_2CH_2, m, 2H), 1.30-1.25 ($CH_2CH_2CH_2CH_2CH_2$, m, 8H), 0.87 (CH_2CH_3, t, *J* = 14.2 Hz, 3H). ^{13}C NMR (125 MHz, $CDCl_3$, ppm): 144.10, 132.12, 128.51, 119.25, 83.97, 76.52, 35.99, 31.88, 31.34, 29.29, 29.24, 22.75, 14.20.

Polymerization

p-*n*-Heptylphenylacetylene (*p*HepPA) was stereoselectively polymerized in *n*Hex using $[Rh(nbd)Cl]_2$ as catalyst and NEt_3 as cocatalyst, affording purple-red poly(*p*HepPA) (Poly(**R**)). In a typical procedure, 600 mg *p*HepPA (3.0 mmol), 14 mg $[Rh(nbd)Cl]_2$ (3.0×10^{-2} mmol), and 0.42 mL NEt_3 (3.0 mmol) were dissolved in 15.0 mL nHex in a specially designed U-shaped flask.[1,4] The polymerization was performed at 25 °C. After 0.5 h, the reaction was quenched with 300 mL MeOH. The polymer was

isolated by filtration, washed with MeOH, and then dried for 24 h at 4 x 10^{-2} torr in a dynamic vacuum.

Poly(**R**) ^{1}H NMR (500 MHz, $CDCl_3$, ppm): 6.67 (br., 2H), 6.52 (br., 2H), 5.78 (br., 1H), 2.36 (br., 2H), 1.45 (br., 2H), 1.25 (br., 8H), 0.87 (br., 3H). ^{13}C NMR (125 MHz, $CDCl_3$, ppm): 141.11, 140.67, 138.86, 131.27, 127.66, 35.85, 32.07, 31.88, 29.84, 29.45, 22.85, 14.25. Anal. Calcd. for $C_{14}H_{18}O$: C, 89.94; H, 10.06. Found: C, 89.56; H, 10.07.

Heat Treatment of Poly(R) at 80 °C

A Poly(**R**) sample was transferred to the bottom of a test tube. While under N_2, the tube was immersed in an 80 °C pre-heated oil bath for 1 h. During the heat treatment, the purple-red Poly(**R**) gradually changed to the black polymer, Poly(**B**).

Measurements

Number and weight average molecular weights (M_n and M_w, respectively) of the polymers were measured at 40 °C using a JASCO GPC 900-1 equipped with two Shodex K-806L columns and a RI detector. Chloroform was used as the eluent, and polystyrene standards (M_n = 800−1,090,000) were employed for calibration. ^{1}H (500 MHz) and ^{13}C (125 MHz) NMR spectra were acquired on a JEOL ECA-500 in $CDCl_3$ at room temperature. Diffuse reflective UV-vis (DRUV-vis) spectra of the polymers were obtained using a JASCO V570 spectrophotometer equipped with an ISN-470 integrating sphere accessory. Wide-angle X-ray diffraction (XRD) patterns of the polymers were recorded on a RIGAKU RINT 2200 Ultima equipped with a heater and a

PTC-30 programmable temperature controller. CuK_{α} radiation was used as the X-ray source. Differential scanning calorimetry (DSC) was performed on a SHIMADZU DSC-60, and samples were run in a N_2 atmosphere using a 10 °C/min heating rate. The thermodynamically favored conformation of *p*HepPA 20-mer was deduced by a molecular mechanics (MM) calculation using the MMFF94 force field (Wavefunction, Inc., Spartan '10 Windows version 1.1.0).[23]

Results and Discussion

Polymerization

The polymerization of *p*HepPA using the Rh complex-NEt_3 catalyst afforded poly(*p*HepPA) (Poly(**R**)) as a purple-red powder in 97 % yield (**Scheme 1**). The yield, number average molecular weight (M_n), polydispersity (M_w/M_n), and the percentage of *cis* carbon-carbon double bonds are listed in **Table 1**. The *cis* % of the polymer was carefully determined using ^{1}H NMR spectra.[1] Previously, we reported that polar, donor organic solvents such as EtOH and NEt_3 induce the dissociation of the Rh catalyst dimer into its catalytically active, solvent-stabilized monomeric species.[1,24] However, to the best of our knowledge, a nonpolar, aprotic, nondonor solvent such as *n*Hex has never been used in this type of polymerization. The decrease of the molecular weight of Poly(**B**) observed after the thermal treatment at 80 °C is substantially correlated to such a stiffness of p-conjugated polymer which induces the main-chain scission.[8(a)]

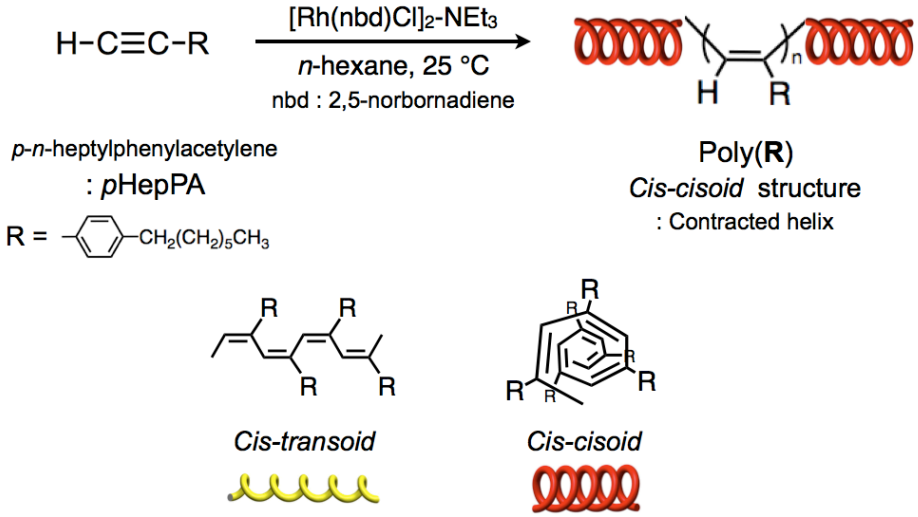

Scheme 1. Synthesis of poly(*p*-*n*-heptyphenylacetylene) having ***contracted*** *cis-cisoid* ***helices***, using [Rh(nbd)Cl]$_2$-NEt_3 catalyst in *n*-hexane.

Table 1. Polymerization of *para*-*n*-heptylphenylacetylene (*p*HepPA) with a $[Rh(nbd)Cl]_2$-NEt_3 catalyst.[a]

Polymer	Solvent	Yield[c] (%)	M_n[d] x10^{-4}	M_w/M_n[d]	*Cis*[e] (%)	Color
Poly(**R**)	*n*-hexane[b]	97	15.1	3.6	87	purple red
Poly(**B**)	HT[f]	-	7.1	3.1	85	black

[a] Polymerization conditions: 25 °C, 30 min, $[M]_0$ = 0.20 M, $[M]_0$/[Rh cat.] = 100, $[NEt_3]$/[Rh cat.] = 100. [b] Polymerization solvent used. [c] MeOH insoluble part. [d] Estimated by GPC analysis (PSt, $CHCl_3$). [e] MeOH insoluble part. Determined by ^1H NMR analysis ($CDCl_3$, r.t.). [f] Prepared by heat treatment (HT) of poly(R) at 80 °C for 1 h under N_2 atmosphere.

Structure of Poly(R) in Solution Detected ^1H NMR

The ^1H NMR spectrum of the purple-red Poly(**R**) was obtained in $CDCl_3$ at room temperature (**Fig. 1**) to determine its molecular geometry. The peaks observed at 6.67, 6.52, 5.78, 2.36, 1.45, 1.25, and 0.87 ppm were assigned to the *meta* protons in a phenyl rings, the *ortho* protons in the phenyl rings, the H-C=C vinyl protons, Ph-C^1H_2, C^2H_2, $(C^{3\sim6})H_8$, and C^7H_3, respectively. The ^1H NMR spectrum of the black Poly(**B**) was almost identical to the spectrum of Poly(**R**) (see Fig. S1). Therefore, no significant differences in chemical shift, line shape, and line width between two polymers were detected in solution phase, despite the large color difference between the solids. Notably, the color of neither polymer faded when the solid chemicals were exposed to air for an

extended time at room temperature. The Poly(**R**) and Poly(**B**) color difference was thus ascribed to morphological or conformational differences, such as in *helical* structure, although SPAs in solution have been considered to take *cis-transoid* structures such as the ***stretched helix*** (***Stretched helix***^{CT}).[8(a)]

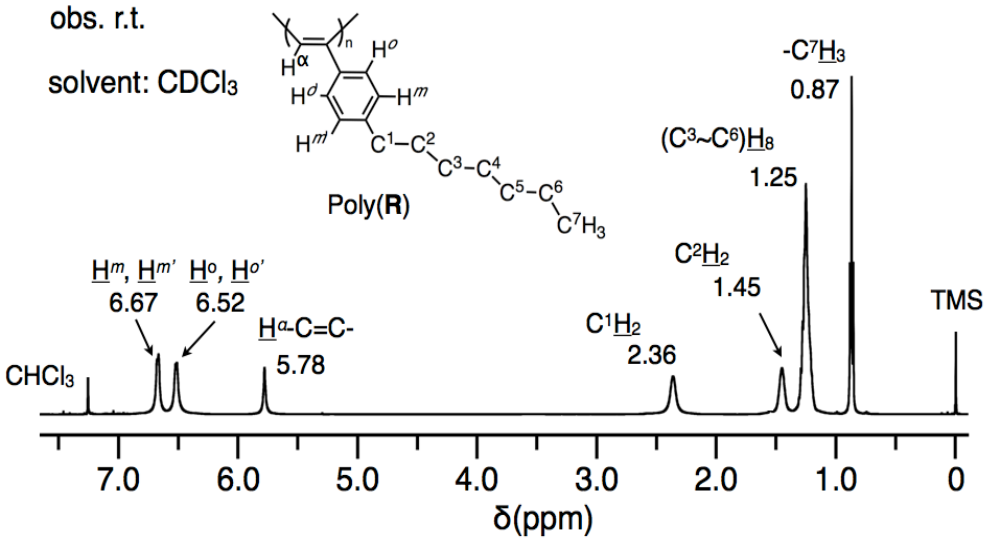

Figure 1. ^{1}H NMR spectra of the purple-red Poly(**R**), observed at room temperature in $CDCl_3$.

Crystal Structure Changes Detected by XRD

To explain the color difference, Poly(**R**) XRD patterns were obtained from room temperature to 140 °C to evaluate temperature dependence (see **Fig. 2**). At room temperature, two primary reflection peaks were observed: one at a low angle side (Bragg distance (d)=24.5 Å) and one at higher angle side (d=4.6 Å). A small peak was also observed at d=3.4 Å. This pattern was analyzed assuming pseudohexagonal crystals with *contracted cis-cisoid helices* (***contracted helices***^{CC}) (**Fig. 3a**). The peak at

d=24.5 Å was attributed to the (100) reflection of the hexagonal crystal. In contrast to the *stretched cis-transoid helices* in the hexagonal crystals of poly(*p*-*n*-hexoxylphenylacetylene) (P*p*HexPA) resulting from using ethanol as the polymerization solvent,[8(a)] this (100) reflection peak indicated that the column diameter (D) of the π-conjugated *helical* column was approximately 28.3 Å (=24.5/sin60°). The large, broad peak at 4.6 Å was attributed to a halo peak superposed on the intramolecular *n*-heptyl alkyl chain distance, as reported previously.[8(a)] The relatively small peak at d = 3.4 Å was attributed to the average intramolecular distance between the *helical* main chain rings and neighboring benzene rings. These results indicated that the ***contracted helices***^{CC} were stabilized in the solid phase.

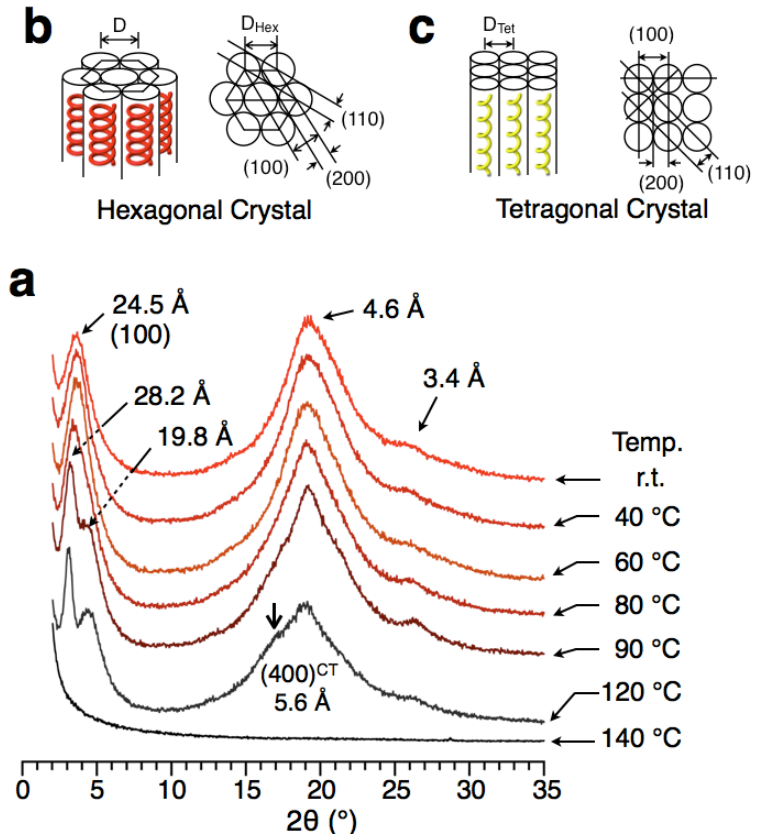

Figure 2. Temperature dependence of the Poly(**R**) XRD patterns.

Additionally, the results indicated that intramolecular π-conjugation, i.e., π-stacking occurred between neighboring phenyl rings or the C=C bonds of the *helical* backbone. The Poly(**R**) peak at d= 24.5 gradually split into two reflection peaks at d=28.2 Å and 19.8 Å when the sample was heated to approximately 80 °C. The half width of the d=28.2 Å peak was small compared with the half width of the d=19.8 Å peak. This difference clearly indicated that the two peaks arose from different crystal structures. The d=28.2 Å peak was ascribed to tetragonal crystals Tet[1] containing *cis-cisoid helices*, whereas the d=19.8 Å peak was ascribed to tetragonal crystals Tet[2] containing *cis-transoid helices*. Therefore, a solid phase *cis-transoid helices*. Therefore, a solid

phase transformation occurred. The Tet[1] peak at d=28.2 Å corresponded to an estimated helical diameter of 28.2 Å (**Fig. 3b**), and the Tet[2] peak at d=19.8 Å (Tet[2] crystals typically contain ***stretched helices***[CT]) corresponded to an estimated helical diameter of 19.8 Å (**Fig. 3c**).

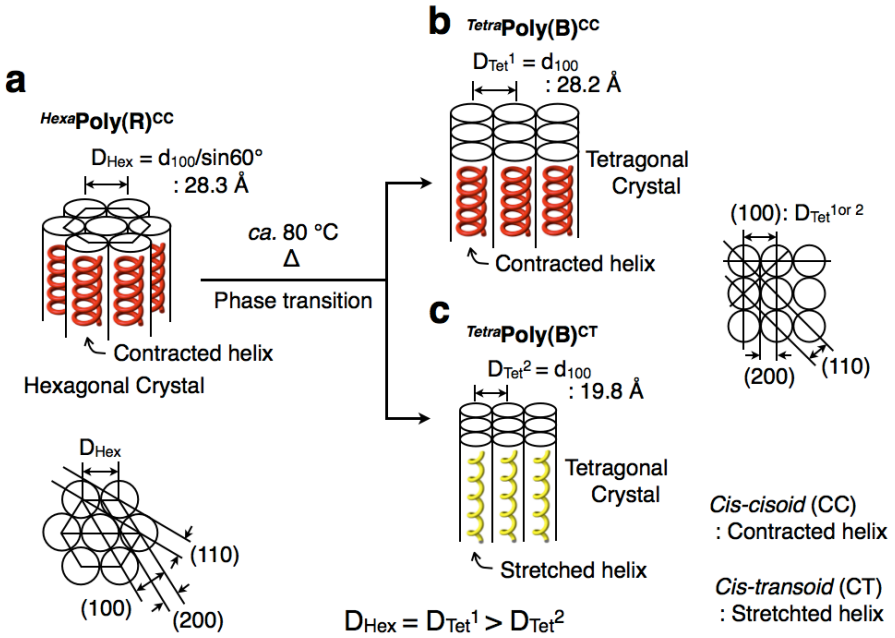

Figure 3. Thermally induced crystal changes accompanied by helical structure changes.

The three peaks decayed completely at approximately 140 °C (**Fig. 2**). These peak disappearances indicated melting of the polymer. The XRD pattern at approximately 80 °C was consistent with the XRD pattern of Poly(**B**), which was obtained by heating Poly(**R**) to approximately 80 °C under N_2. These results indicated that Poly(**B**) was composed of two tetragonal crystals in which different helices, i.e., ***contracted helices***[CC] and ***stretched helices***[CT], are packed in the solid columnar phase. Formation of

the D=28.2 Å tetragonal crystal resulted in the 3.4 Å peak remaining until 120 °C.

Table 2. Column diameters determined by XRD spectra and molecular mechanics calculations.

Polymer	Temp. (°C)	Lattice	d_{100}[a] (Å)	$D_{obs.}$ (Å)	$D_{calc.}$[c] (Å)
Poly(**R**)	r.t.	Hexagonal	24.5	28.3[b]	28.3
Poly(**B**)	90	Tetragonal	28.2	28.2	28.3
Poly(**B**)	90	Tetragonal	19.8	19.8	20.1

[a] Determined by XRD analysis. [b] $d_{100}/\sin 60°$. [c] Determined by molecular mechanics (MM) calculations used a MMFF 94 force field program.

Moreover, the relatively broad reflection peak at d=19.8 Å was attributed to the (100) reflection of the Tet^{2} crystal, which contained ***stretched helices***^{CT}. For tetragonal crystals, the helical diameter corresponds to the length derived from the (100) reflection peak (**Figs. 2** and **3**); therefore, the helical diameter for Tet^{2} was calculated as approximately 19.8 Å. This assignment was supported by the small peak at d=5.6 Å because this peak was consistent with a (400) reflection of Tet^{2} crystals containing D=19.8 Å ***stretched helices***^{CT}. The change in XRD pattern with temperature indicated that the pristine ^{Hexa}Poly(**R**)^{CC} (hexagonal crystals comprising *cis-cisoid* helices) was thermodynamically unstable relative to ^{Tetra}Poly(**B**)^{CC} (tetragonal crystals comprising *cis-cisoid* helices) and ^{Tetra}Poly(**B**)^{CT} (tetragonal crystals comprising *cis-transoid* helices).

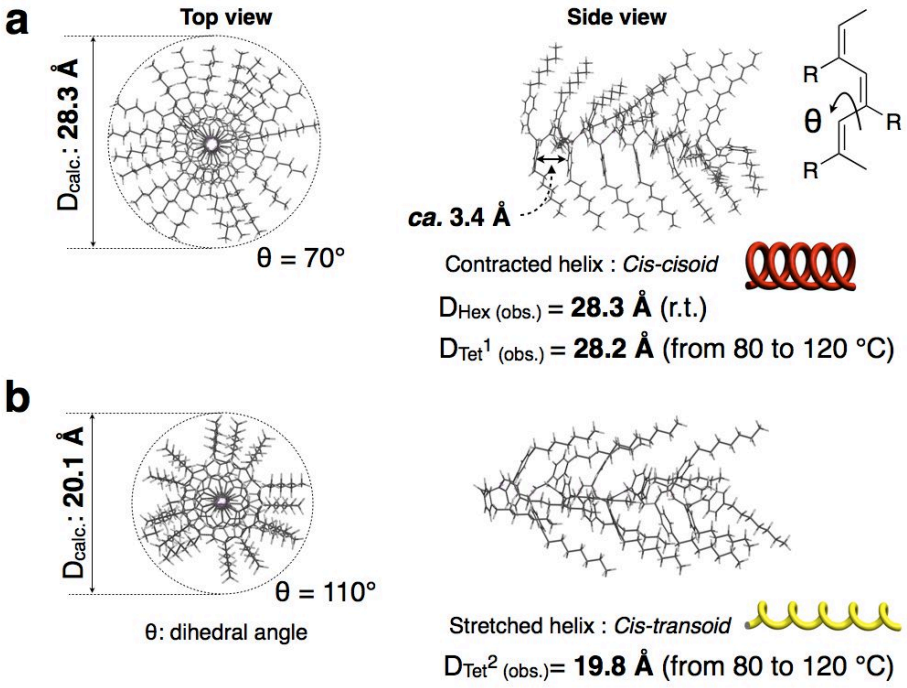

Figure 4. Top and side views of *cis-cisoid* and *cis-transoid* helices calculated using the MMFF94 force field.

In summary, heating induces an important solid phase rearrangement from pristine hexagonal crystals to two types of tetragonal crystals: Tet^{1} and Tet^{2}. Tet^{1} contains identical *cis-cisoid* helices to the pristine hexagonal crystal, and Tet^{2} contains *cis-transoid* helices (**Figs. 3** and **4**).[8(a)]

Molecular Mechanics Calculation

The most stable helical conformations of ^{Hexa}Poly(**R**)^{CC}, ^{Tetra}Poly(**B**)^{CC}, and ^{Tetra}Poly(**B**)^{CT} were simulated using the *p*HepPA 20-mer as a model. The molecular mechanics (MM) calculations used a MMFF 94 force field program.[23] The MMFF 94 calculations were performed by rotating the dihedral angles (θ) about the C-C single

bonds in the C=C-C=C moieties. These calculations afforded the relationship between θ (°) and the strain energy (kJ/(unit mol)) (**Figs. 4 and 5**). These results clearly demonstrated that the strain energy was minimized (119.0 kJ/(unit mol)) at approximately θ = 110°, in agreement with the angle calculated using the helical diameter D=20.1 Å and assuming a hexagonal helix (see **Fig. 4**). Moreover, the dihedral angle θ=70° corresponded to the strain energy of the *cis-cisoid helix*, and the helical diameter calculated from that dihedral angle was consistent with the helical diameter (28.3 Å) obtained from XRD data. These data support the assertion that the unstable *cis-cisoid helix* is easily produced in *n*-hexane but partly transformed to the considerably more stable *cis-transoid* helix upon heating to 80 °C. The π-stacking distance corresponded to the *helical* pitch in the 20-mer model polymers of ^{Hexa}Poly(**R**)^{CC} and ^{Tetra}Poly(**B**)^{CC}, and the MMFF 94 calculation of approximately 3.4 Å was consistent with XRD results. Additionally, the lengths of the *cis-cisoid* helices, which were experimentally deduced using XRD peak widths, were at least 100 Å, i.e., a relatively large value.

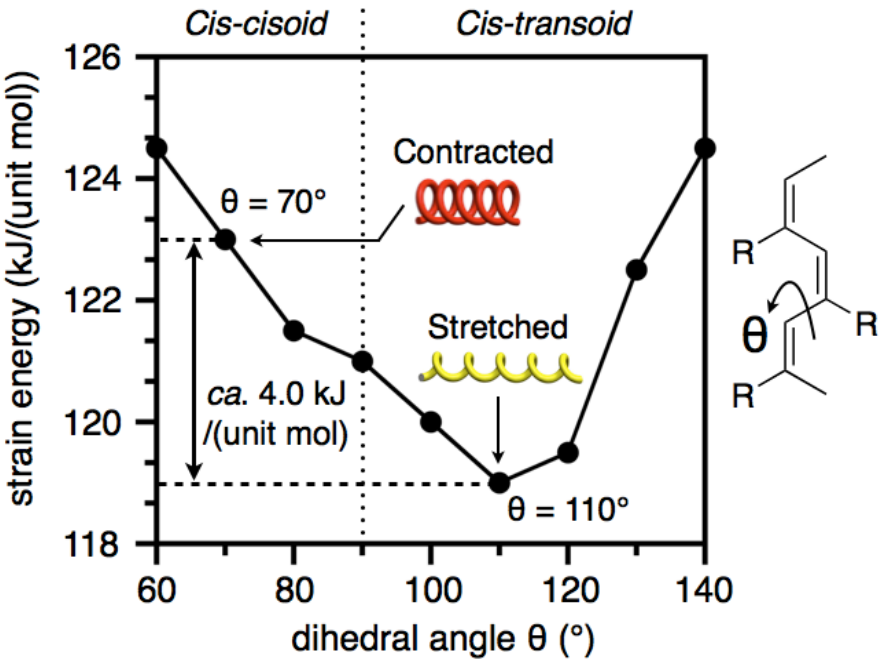

Figure 5. Strain energy dependence on the C=C-C=C dihedral angles as calculated by the MMFF94 force field program.

DSC Studies

Fig. 6 shows the DSC trace of ^{Hexa}Poly(**R**)^{CC} measured under nitrogen from 30 to 200 °C at the heating rate of 10 °C/min. The trace exhibited three endothermic peaks at approximately 40, 75, and 85 °C and a large exothermic peak at approximately 150 °C. The third endothermic peak at approximately 85 °C was attributed to the solid phase transition from pristine hexagonal crystals comprising *cis-cisoid helices* to Tet^{1} tetragonal crystals comprising *cis-cisoid helices* and Tet^{2} tetragonal crystals comprising ***stretched helices***^{CT} having the *cis-transoid* helix. The small endotherms at approximately 40 and 75 °C (**Fig. 6b**) were attributed to the melt or reorientation of the *n*-heptyl alkyl side chains. Notably, the thermal treatment of Poly(**B**) under N_2 for 1 h at

temperatures higher than 140 °C rapidly decreased the *cis* % because of isomerization, as evinced by the DSC trace (**Fig. 6**). The enthalpy of transition energy (DH≈0.89 kJ/(unit mol)) corresponded to the thermally induced rearrangement of ^{Hexa}Poly(**R**)^{CC} to ^{Tetra}Poly(**B**)^{CC} and ^{Tetra}Poly(**B**)^{CT}, although the enthalpy from the small endothermic peak at 70 °C is included in this value. This enthalpy value was approximately 1/5 of the calculated 4.0 kJ/(unit mol) obtained from the MMFF 94 method (**Fig. 5)**. This inconsistency was rationalized in terms of column structure. Because both the rotational angles about the main-chain and the positioning of the long alkyl chains require changing, i.e., the solid phase transition of ^{Hexa}Poly(**R**)^{CC} to ^{Tetra}Poly(**B**)^{CC} and ^{Tetra}Poly(**B**)^{CT} requires a large amount of energy. Therefore, the thermally induced rearrangement did not proceed smoothly. In other words, less than 1/5 of the helical components in ^{Hexa}Poly(**R**)^{CC} rearranged to ^{Tetra}Poly(**B**)^{CC} and ^{Tetra}Poly(**B**)^{CT} in the solid phase.

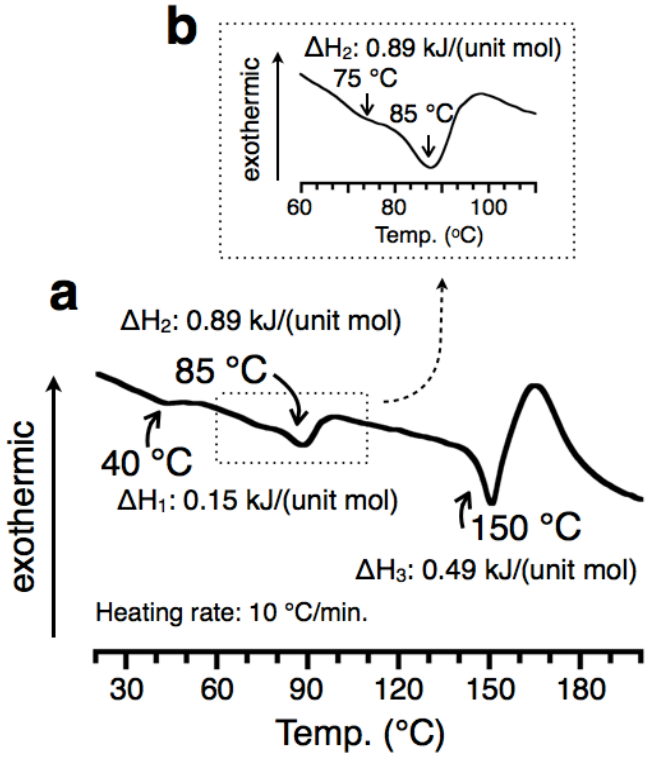

Figure 6. DSC traces of ^{Tetra}Poly(**R**)^{CC} from 30 °C to 200 °C under N_2.

Solid Phase DRUV-Vis Spectra

The DRUV-Vis spectra of ^{Hexa}Poly(**R**)^{CC} were obtained before and after the heat treatment (**Figs. 7a** and **b**). The absorption spectrum of ^{Hexa}Poly(**R**)^{CC} exhibited two maxima (λ_{max}) at 292 and 482 nm and an extremely long absorption tail until approximately 1100 nm. The absorption at approximately 482 nm was attributed to the *cis-cisoid helices* within ^{Hexa}Poly(**R**)^{CC}.[8(a)] Previously, *cis* and *trans* polyacetylenes with no substituents were prepared using the Ziegler-Natta catalyst Et_3Al-Ti(O*n*-Bu)$_4$ and had λ_{max} at 570 and 675 nm with small shoulders at approximately 500 and 600 nm, respectively.[25] The λ_{max} at 482 nm in ^{Hexa}Poly(**R**)^{CC} shifted to 560 nm when heated at

approximately 80 °C for 1 h. This observation indicated that the helical pitch shortened to accommodate ordered π-stacking along the helical backbone. The large absorption at 294 nm with a relatively narrow width was also attributed to shorter *cis-cisoid helices* or distorted *cis-cisoid helices* that were generated during the original polymerization in *n*-hexane. Therefore, polymerization in *n*-hexane produced helices with both long and short pitches. To the best of our knowledge, however, the long absorption tail extending into the near infrared region, i.e., more than 1100 nm is neither explained by π-stacking nor reported in other π-conjugated polymers.[26] Poly(phenylacetylene) (PPA) prepared using the Ziegler–Natta catalyst $Fe(acac)_3$-$AlH(i\text{-}Bu)_2$ was red and insoluble.

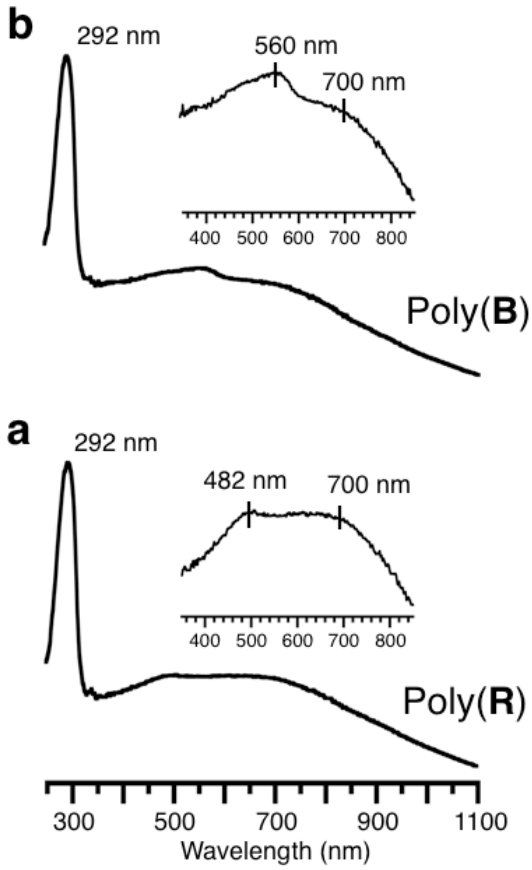

Figure 7. DRUV-vis spectra of Poly(**R**) and Poly(**B**) observed on alumina powder.

Poly(*p*-methylphenylacetylene) (PMPA) prepared with a Rh catalyst was also red and insoluble.[8(c)] Therefore, the physical properties of those previous PPAs interfered with detailed structural analyses.

Importance of PPA Including P*p*HepPA with a Contracted Helical Pitch

SPAs, including the present PPA, are some of the stiffest *helical* polymers because they are composed of alternating C-C and C=C conjugated bonds and possess additional p-conjugation from π-stacking in the direction of the molecular backbone.[8] The calculated *helical* pitch of ^{Hexa}Poly(**R**)^{CC} and ^{Tetra}Poly(**B**)^{CC} was approximately 3.4 Å (**Table 2**) and was comparable to the layer distance of electrically conductive graphite, 3.35 Å and graphene.[27] For poly(ethyl propiolate) (PEP), the vertical electric current of a single *helix* was measured as approximately 10^{-8} A without doping, and it was the smallest semi-conductor using such a *helical* polymer.[28]

Conclusion

p-*n*-Heptylphenylacetylene (*p*HepPA) was stereoregularly polymerized at 25 °C using $[Rh(nbd)Cl]_2$ and NEt_3 in *n*-hexane, affording the purple-red polymer Poly(R) in high yield. Poly(R) transformed into the black polymer Poly(B) upon heating to 80 °C. Both polymers were analyzed by XRD, MMFF 94 calculations, DSC, and DRUV-vis. In solid-phase DRUV-vis, Poly(R) and Poly(B) exhibited absorption maxima (l_{max}) at 482 and 560 nm, respectively. No significant differences were observed in ^{1}H NMR when the spectra were obtained in chloroform. The XRD patterns of Poly(R) revealed

that it had a hexagonal crystal structure (^{Hexa}Poly(R)) comprising *cis-cisoid helices* (*i.e., contracted helices* called ^{Hexa}Poly(R)^{CC}). Furthermore, heating Poly(R) up to 120 °C induced the solid phase transformation of ^{Hexa}Poly(R)^{CC} to two tetragonal crystal phases: one containing large-diameter *cis-cisoid helices* and the other containing small-diameter *stretched helices*. Moreover, the thermally induced rearrangement of ^{Hexa}Poly(R)^{CC} to the black polymers ^{Tetra}Poly(B)^{CC} and ^{Tetra}Poly(B)^{CT} occurred at approximately 80 °C. To the best of our knowledge, a solid phase rearrangement resulting from a *contracted helix*^{CC} to a stretched *helix*^{CT} transformation and accompanied by a drastic color change has never been reported. The thermal instability of ^{Hexa}Poly(R)^{CC} was proven by the DSC endotherm at approximately 80 °C. These data clearly corroborated that the pristine ^{Hexa}Poly(R)^{CC} crystals thermally converted into the two tetragonal crystals containing *contracted helices*^{CC} and stretched *helices*^{CT} at approximately 80 °C. The origin of the color changes observed before and after the heat treatment is attributed to the helical pitch width and the increment of intramolecular π-stack order i.e., the degree of π-conjugation in the vertical direction of the main chain of the contracted *helix* packed in the *tetragonal* crystal 1 as indicated by the large red shift of the l_{max} from 482 nm to 560nm in the DRUV-vis spectrum.

Reference

1. (a) M. Tabata, W. Yang, K. Yokota, *Polym. J.* **1990**, 22, 1105-1107. (b) W. Yang, M. Tabata, K. Yokota, *Polym. J.* **1991**, 23, 1135-1138. (c) M. Tabata, W. Yang, K. Yokota, *J. Polym. Sci. Part A: Polym. Chem.* **1994**, 32, 1113-1120. (d)

M. Lindgren, H. S. Lee, W. Yang, M. Tabata and K. Yokota, *Polymer* **1991**, 32, 1532–1534. (e) Y. Yoshida, Y. Mawatari, C. Seki, T. Hiraoki, H. Matsuyama, M. Tabata, *Polymer* **2011**, 52, 646-651.

2. (a) Y. Kishimoto, P. Eckerle, T. Miyataka, M. Kainosho, A. Ono, T. Ikariya, R. Noyori, *J. Am. Chem. Soc.* **1999**, 121, 12035-12044. (b) N. Onishi, M. Shiotsuki, F. Sanda, T. Masuda, *Macromolecules* **2009**, 42, 4071-4076. (c) T. Nishimura, Y. Ichikawa, T. Hayashi, N. Onishi, M. Shiotsuki, T. Masuda, *Organometallics* **2009**, 28, 4890-4893. (d) M. Shiotsuki, N. Onishi, F. Sanda, T. Masuda, *Chem. Lett.* **2010**, 244-245. (e) M. Shiotsuki, F. Sanda, T. Masuda, *Polym. Chem.* **2011**, 2, 1044-1058. (f) W. Zhang, J. Tabei, M. Shiotsuki, T. Masuda, *Polym. Bull.* **2006**, 57, 463-472.
3. A. Nakazato, I. Saeed, T. Katsumata, M. Shiotsuki, T. Masuda, J. Zednik, J. Vohlidal, *J. Polym. Sci. Part A: Polym. Chem.* **2005**, 43, 4530–4536.
4. M. Tabata, S. Kobayashi, Y. Sadahiro, Y. Nozaki, K. Yokota, W. Yang, *J. Macromol. Sci. Pure. Appl. Chem.* **1997**, A34(4), 641–653.
5. (a) E. Yashima, T. Matsushima, Y. Okamoto, *J. Am. Chem. Soc.* **1995**, 117, 11596–11597. (b) K. Maeda, H. Goto, E. Yashima, *Macromolecules* **2001**, 34, 1160–1164. (c) R. Nomura, Y. Fukushima, H. Nakako, T. Masuda, *J. Am. Chem. Soc.* **2000**, 122, 8830–8836. (d) R. Nomura, H. Nakako, T. Masuda, *J. Mol. Catal. A: Chem.* **2002**, 190, 197–205. (e) E. Yashima, K. Maeda, H. Iida, Y. Furusho, K. Nagai, *Chem. Rev.* **2009**, 109, 6102–6211.
6. (a) F. Sanda, T. Masuda, *J. Synth. Org. Chem., Jpn.* **2008**, 66, 757–764. (b) M.

Shiotsuki, F. Sanda, T. Masuda, *Polym. Chem.* **2011**, 2, 1044–1058. (c) T. Aoki, T. Kaneko, M. Teraguchi, *Polymer* **2006**, 47, 4867–4892. (d) F. Freire, J. M. Seco, E. Quiñoá, R. Riguera, *J. Am. Chem. Soc.* **2012**, 134, 19374−19383. (e) L. Liu, Y. Zang, S. Hadano, T. Aoki, M. Teraguchi, T. Kaneko, T. Namikoshi, *Macromolecules* **2010**, 43, 9268-9276.

7. M. Kozuka, T. Sone, Y. Sadahiro, M. Tabata, T. Enoto, *Macromol. Chem. Phys.* **2002**, 203, 66-70.
8. (a) A. Motoshige, Y. Mawatari, Y. Yoshida, C. Seki, H. Matsuyama, M. Tabata, *J. Polym. Sci. Part A: Polym. Chem.* **2012**, 50, 3008–3015. (b) Y. Mawatari, M. Tabata, *J. Jpn. Soc. Colour Mater* **2009**, 82, 204–209. (c) Y. Mawatari, M. Tabata, T. Sone, K. Ito Y. Sadahiro, *Macromolecules* **2001**, 34, 3776–3782.
9. T. Masuda, E. Isobe, T. Higashimura, K. Takada, *J. Am. Chem. Soc.* **1983**, 105, 7473-7474.
10. (a) D. Neher, A. Wolf, C. Bubeck, G. Wegner, *Chem. Phys. Lett.* **1989**, 163, 116-122. (b) J. L. Bredas, C. Adant. P. Tacks, A. Persoons, M. Pierce, *Chem. Rev.* **1994**, 94, 243-278. (c) M. Falconieri, R. D'Amato, M. V. Russo, A. Furlani, *Nonlinear Opt.* **2001**, 27, 439-442. (c) M. Tabata, T. Sone, K. Yokota, T. Wada, H. Sasabe, *Nonlinear Opt.* **1999**, 22, 341-344. (d) T. Wada, L. Wang, H. Okawa, T. Masuda, M. Tabata, M. Wan, M. Kakimoto, Y. Imai, H. Sasabe, *Mol. Cryst. Liq. Cryst.* **1997**, 294, 245-250.
11. (a) T. A. Skotheim, ed, Handbook of Conducting Polymers; Dekker, E.D: New York, 1986; vol. 1–2. (b) J. R. Ferraro, J. M. Williams, Introduction to Synthetic.

Electrical Conductors, E. D.; Academic Press Inc.: New York, 1987. (c) J. C. Salomone, Polymeric Materials, E. D.; d. CRC Press: New York, 1996, vol. 8.

12. (a) Y. V. Korshak, T. V. Medvedeva, A. A. Ovchinnikov, V. Spector, *Nature* **1987**, 326, 370-372. (b) N. Tyutyulkov, K. Müllen, M. Baumgarten, A. Ivanova, A. Tadjer, *Synth. Met.* **2003**, 139, 99-107. (c) M. Tabata, Y. Nozaki, W. Yang, K. Yokota, Y. Tazuke, *Proc. Jpn. Acad.* **1995**, 71, 219-224. (d) K. H. Fisher, J. A. Herz, Spin glass; Cambridge University Press: Cambridge, 1991, 30. (e) J. J. Pregjean, J. Souletie, *J. Phys.* **1980**, 41, 1335-1352. (f) L. Floch, F. Hammann, J. Ocio, M. Vincent, *Euro. Phys. Lett.* **1992**, 18, 647-652. (g) D. G. Xenikos, H. Multer, C. Jouan, A. Suilpice, J. L. Tholence, *Solid State Commun.* **1997**, 102, 681-685. (h) M. Tabata, Y. Watanabe, S. Muto, *Macromol. Chem. Phys.* **2004**, 205, 1174-1178. (i) Y. Watanabe, S. Muto, M. Tabata, *Jpn. J. Appl. Phys. Part 2 Lett.* **2004**, 43, 300-302.
13. K. Maeda, E. Yashima, *J. Synth. Org. Chem. Jpn.* **2002**, 60, 878–890.
14. (a) E. Yashima, T. Matsushima, Y. Okamoto, *J. Am. Chem. Soc.* **1995**, 117, 11596–11597. (b) K. Maeda, H. Goto, E. Yashima, *Macromolecules* **2001**, 34, 1160–1164. (c) R. Nomura, Y. Fukushima, H. Nakako. T. Masuda, *J. Am. Chem. Soc.* **2000**, 122, 8830–8836. (d) R. Nomura, H. Nakako, T. Masuda, *J. Mol. Catal A: Chem.* **2002**,190, 197–205. (e) E. Yashima, K. Maeda, H. Iida, Y. Furusho and K. Nagai, *Chem. Rev.* **2009**, 109, 6102–6211.
15. R. J. Kern, *J. Polym. Sci., Polym. Chem. Ed.* **1969**, 7, 621-631.
16. T. Masuda, T. Higashimura, *Adv. Polym. Sci.* **1986**, 81, 121.

17. (a) T. Sone, R. Amato, Y. Mawatari, M. Tabata, A. Furlani, M. V. Russo, *J. Polym. Sci. Part A: Polym. Chem.* **2004**, 42, 2365-2376. (b) C. I. Shimionescu, V. Percec, S. Dumitrescu, *J. Polym. Sci: Polym. Chem. Ed.* **1977**, 2497-2509. (c) R. D'Amato, T. Sone, M. Tabata, Y. Sadahiro, M. V. Russo, A. Furlani, *Macromolecules* **1998**, 31, 8660-8665.

18. (a) T. Sone, R. Asako, T. Masuda, M. Tabata, T. Wada, H. Sasabe, *Macromolecules* **2001**, 34, 1586-1592. (b) A. Miyasaka, M. Nakamura, Y. Mawatari, K. Orito, M. Tabata, *Macromol. Symp.* **2006**, 239, 13-20. (c) E. Sato, Y. Mawatari, Y. Sadahiro, B. Yamada, M. Tabata, Y. Kashiwaya, *Polymer* **2008**, 49, 1620-1628.

19. (a) V. Percec, G. J. Rudick, M. Peterca, M, Wagnar, M. Obata, M. C. Mitchell, W. Cho, S. K. V. Balagurusamy, A. P. Heiney, *J. Am. Chem. Soc.* **2005**, 127, 15257-15264. (b) V. Percec, G. J. Rudick, M. Peterca, A. P. Heiney, *J. Am. Chem. Soc.* **2008**, 130, 7503-7508.

20. (a) T. Aoki, T. Kaneko, N. Maruyama, A. Sumi, M. Takahashi, T. Sato, M. Teraguchi, *J. Am. Chem. Soc.* **2003**, 125, 6346−6347. (b) S. Hadano, T. Kishimoto, T. Hattori, D. Tanioka, M. teraguchi, T. Aoki, T. Kaneko, T. Namikoshi, E. Marwanta, *Macromol. Chem. Phys.* **2009**, 210, 717-727. (c) L. Liu, T. Namikoshi, Y. Zang, T. Aoki, S. Hadano, Y. Abe, I. Wasuzu, T. Tsutsuba, M. Teraguchi, T. Kaneko, *J. Am. Chem. Soc.* **2013**, 135, 602−605.

21. (a) Y. Yoshida, Y. Mawatari, A. Motoshige, R. Motoshige, T. Hiraoki, M. Wagner, K. Müllen, M. Tabata, *J. Am. Chem. Soc.* **2013**, 135, 4110-4116. (b) Y.

Yoshida, Y. Mawatari, A. Motoshige, R. Motoshige, T. Hiraoki, M. Tabata, P*olym. Chem.* **2013**, 4, 2982-2988.

22. S. Ito, M. Wehmeier, J. Brand, C. Kübel, R. Epsch, J. Rabe, K. Müllen, *Chem. Eur. J.* **2000**, 6, 4327-4342.
23. MMFF94 calculations were carried out with a Spartan'10 (Windows version 1.1.0), Wavefunction, Inc, California.
24. A. Nakazato, I. Saeed, T. Katsumata, M. Shiotsuki, T. Masuda, J. Zednik, J. Vohlidal, *J. Polym. Sci. Part A: Polym. Chem.* **2005**, 43, 4530–4536.
25. M. Tabata, T. Sone, Y. Sadahiro, *Macromol. Chem. Phys.* **1999**, 200, 265–282.
26. K. Takagi, Y. Nishikawa, N. Nishioka, H. Kunisada, Y. Yuki, *J. Polym. Sci. Part A: Polym. Chem.* **2002**, 40, 3927-3937.
27. I. L. Spain, The physics of semimetals and narrow band-gap semiconductors carter; D. L. Carter and R. T. Bate, E. D.; Pergamon Press Oxford: Oxford ,1971.
28. (a) O. Albrecht, T. Sone, A. Kuriyama, K. Eguchi, K. Yano, *Nanotechnology* **2008**, 19, 505201. (b) N. Wang, Y. Zhang, K. Yano, C. Durkan, N. Plank, M. E. Welland, H. E. Unalan, M. Mann, G. A. J. Amaratunga, W. I. Milne, *Nanotechnology* **2009**, 20, 105201.

Chapter 3

Synthesis and Solid State *Helix* to *Helix* Rearrangement of Poly(phenylacetylene) Bearing *n*-Octyl Alkyl Side Chains

Abstract

Highly stereoregular polymerisations of *p*-*n*-octyphenylacetylene (*p*OcPA) were performed using a [Rh(norbornadine)Cl]$_2$-triethylamine catalyst in ethanol at -20 and 25 °C to afford yellow and orange polymers, Poly(**Y**) and Poly(**O**), in yields of 64 and 99%, respectively. The XRD patterns of Poly(**Y**) showed a *hexagonal* columnar liquid crystal with a ***contracted*** *cis-cisoid* helix, ^{Hexa}Poly(**Y**)^{CC}. The XRD pattern of Poly(**O**) matched that of Poly(**Y**) heated to 80 °C. The heat treatment of ^{Hexa}Poly(**Y**)^{CC} at 100 °C generated two *tetragonal* crystals: ^{Tetra1}Poly(**R**)^{CC}, containing ***contracted*** *cis-cisoid* helices and ^{Tetra2}Poly(**R**)^{CT}, containing ***stretched*** *cis-transoid* helices. The *helical* diameters of ^{Hexa}Poly(**Y**)^{CC} before and after heat treatment were estimated using XRD and were consistent with the results of MMFF 94 calculations, although the *n*-octyl alkyl chains of ^{Hexa}Poly(**Y**)^{CC} and ^{Tetra2}Poly(**R**)^{CT} did not have a linear alkyl chains; a bent in the chains was confirmed by ^{13}C CP-MAS NMR. When ^{Hexa}Poly(**Y**)^{CC} was heated to 100 °C in the solid phase, the λ_{max} in the diffuse reflective UV-vis spectra shifted from 448 nm to 565 nm. Furthermore, the endothermic transition for ^{Hexa}Poly(**Y**)^{CC} occurred at 100 °C in the DSC trace. Therefore, these data corroborated the assertion that ^{Hexa}Poly(**Y**)^{CC} thermally converted to ^{Tetra1}Poly(**R**)^{CC} and ^{Tetra2}Poly(**R**)^{CT}.

Introduction

Polyacetylenes (PA)s and mono-substituted polyacetylenes (SPA)s typical for conjugated polymers have been prepared using various catalysts, such as the Ziegler-Natta catalyst, $Fe(acac)_3$-$AlH(i\text{-}Bu)_2$[1]; the Luttinger catalyst, $(n\text{-}Bu_3P)_2NiCl_2$-$NaBH_4$[2]; $RhCl_3$-$LiBH_4$[1]; the Wilkinson catalyst, $RhCl(PPh_3)_3$[1]; metathesis catalysts, such as WCl_6 or $MoCl_5$[3]; bidentate Rh catalysts, $[Rh(nbd)Cl]_2$-cocatalyst (nbd=norbornadiene)[4]; and zwitterionic mono Rh complex catalysts.[5] Among them, the Rh bidentate catalyst has become an important catalyst for the synthesis of *helical* SPAs with *cis-transoid* geometrical structures from various mono-substituted acetylene (SA) monomers. A monodentate Rh complex has been reported as the active catalyst, and this species is generated *in situ* from the Rh bidentate catalyst when triethylamine (TEA), alcohol, or aqueous alcohols are used as the cocatalyst or solvent.[4a-4e] The *cis-transoid helices* are driven by van der Waals forces to produce a columnar liquid crystal called a *hexagonal* columnar crystals as the assembly of the *helical* main chain in the solid phase.[6,7]

The *helical* pitch of an alkoxy substituted poly(phenylacetylene) was controlled using external stimuli.[8] For example, thermal treatment of the solid converts the ***stretched*** *cis-transoid helices* to ***contracted*** *cis-cisoid helices*, and this transformation is accompanied by a drastic colour change from bright yellow to dark red.[8a] However, the morphology of these polymers and the mechanism of the solid phase transformation have not been thoroughly investigated despite the many interesting physicochemical properties of the polymer, including oxygen permeability,[6b,9] nonlinear optical

behaviour,[10] electrical conductivity,[11] time and temperature memory,[12] enantioselectivity,[13] and response to external stimuli.[14]

Recently, the chiral side-chain induced formation of predominantly one-handed SPA *helices* was explained by CD spectral data, which were also used to explain the dynamic *helix* inversions.[15,16] Poly(phenylacetylene)s (PPAs) prepared using the Ziegler-Natta[1] and metathesis catalysts[3] have interfered with the geometrical and spatial structure of the polymers. These interferences occurred because of the presence of gels, large quantities of irregular sequences, (i.e., *head*-to-*head* and/or *tail*-to-*tail* bond units), or unpaired electrons present in the polymers. The unpaired electrons were generated through the rotational scission of *cis* C=C bonds[17] by thermal *cis*-to-*trans* isomerisation,[17(b)] and compression,[17(c)] and even during polymerisation.[17(d,e)]

In Chapter 2, we found that poly(*p*-*n*-heptylphenylacetylene) transformed from *contracted helix* to *stretched helix* by the heat-treatment. Moreover, we showed that the columnar structure changed from hexagonal crystal to tetragonal crystal. In this Chapter, we used *p*-*n*-octylphenyacetylene as an another monomer. We found an important experimental conditions to change such helical pitch and crystal structure.

In this report, *p*-*n*-octylphenylacetylene (*p*OcPA) was polymerised in ethanol at -20 °C using the Rh complex catalyst with TEA as the cocatalyst affording the bright yellow poly(*p*OcPA), ^{Hexa}Poly(**Y**)^{CC}, which was a *hexagonal* columnar crystal with ***contracted*** *cis-cisoid helices*. Moreover, we report a solid state *helix to helix* rearrangement from ^{Hexa}Poly(**Y**)^{CC} to two *tetragonal* crystals when heated from 30 °C to 100 °C: Tetra[1] with ***contracted*** *cis-cisoid* helices, ^{Tetra1}Poly(**R**)^{CC}, and Tetra[2] with

stretched *cis-transoid* helices, ^{Tetra2}Poly(**R**)^{CT}. The *n*-octyl alkyl chains of ^{Hexa}Poly(**Y**)^{CC} and ^{Tetra2}Poly(**R**)^{CT} do not have extended alkyl chains but have bent chains. Furthermore, determining if the ***contracted*** *cis-cisoid helices* (***contracted*** *helix*^{CC}) generated are energetically stable structures is important. Because the ***contracted*** *helix*^{CC} was considered to be a missing helix for a long time and was only recently identified in the solid phase and in solution, in which an interesting ***Accordion-like Helix Oscillation*** **(*HELIOS*)** of achiral and chiral aliphatic polyacetylene is shown.[18] Therefore, the morphologies and geometric structures of Poly(**Y**) before and after thermal treatment were carefully determined using ^{1}H and ^{13}C NMR spectroscopies, wide angle X-ray diffraction (XRD), differential scanning calorimetry (DSC), solid phase UV-vis spectroscopy, molecular mechanics calculations (MMFF 94 force field), and solid state ^{13}C CP-MAS NMR methods.

Experimental Section

Materials

Ethanol (EtOH), and triethylamine (TEA) (JUNSEI Chemical Co.) were distilled before use. $[Rh(nbd)Cl]_2$ (nbd = norbornadiene) was purchased from Aldrich and used without further purification.

Monomer Synthesis

The $[Rh(nbd)Cl]_2$ (nbd = norbornadiene) catalyst was purchased from Aldrich and used without further purification. The monomer, *p*-*n*-octylphenylacetylene (*p*OcPA), was prepared according to a literature procedure[19] and purified by silica gel column chromatography using *n*-hexane as an eluent. ^{1}H NMR (500 MHz, $CDCl_3$, ppm): 6.67 (Ph-*H*, d, *J* = 8.2 Hz, 2H), 6.51 (Ph-*H*, d, *J* = 8.3 Hz, 2H), 3.03 (*H*-C≡C, s, 1H), 2.59 (Ph-CH_2, t, *J* = 15.6 Hz, 2H), 1.60-1.57 (CH_2CH_2, m, 2H), 1.29-1.26 ($CH_2CH_2CH_2CH_2CH_2$, m, 10H), 0.88 (CH_2CH_3, t, *J* = 14.1 Hz, 3H). ^{13}C NMR (125 MHz, $CDCl_3$, ppm): 144.13, 132.18, 128.55, 119.35, 84.03, 76.56, 36.05, 32.02, 31.38, 29.59, 29.39, 29.39, 22.82, 14.25.

Polymerisation

*p*OcPA was polymerised in EtOH using $[Rh(nbd)Cl]_2$ as the catalyst and TEA as the cocatalyst to afford bright yellow poly(*p*OcPA), (Poly(**Y**)). In a typical procedure, 500 mg of *p*OcPA (2.3 mmol), 10 mg of $[Rh(nbd)Cl]_2$ (2.3×10^{-2} mmol), and 0.32 mL of TEA (2.3 mmol) were dissolved in 11.7 mL of EtOH in a specially designed U-shaped

flask.[4a-4e] The polymerisations were performed at -20°C and 25 °C. After 0.5 h, the reaction was quenched with 300 mL of MeOH. The polymers were isolated by filtration, washed with MeOH and then dried for 24 h at 4 x10^{-2} torr in a dynamic vacuum. The polymerisations at -20 °C and 25 °C afforded a bright yellow polymer, Poly(**Y**), and an orange polymer, Poly(**O**), as powders with yields of 64 % and 99 %, respectively: ^{1}H NMR (500 MHz, $CDCl_3$, ppm): 6.67 (br., 2H), 6.51 (br., 2H), 5.78 (br., 1H), 2.36 (br., 2H), 1.45 (br., 2H), 1.25 (br., 10H), 0.88 (br., 3H). ^{13}C NMR (125 MHz, $CDCl_3$, ppm): 141.16, 140.74, 138.95, 131.32, 127.71, 127.71, 35.92, 32.16, 31.93, 29.98, 29.81, 29.62, 22.89, 14.28. Anal. Calcd. for C16H22: C, 89.65; H, 10.35. Found: C, 89.32; H, 10.35.

Heat Treatment of Poly(Y) at 80 and 100 °C

A sample of Poly(**Y**) was placed at the bottom of a test tube and the tube was immersed in a pre-heated oil bath for 1 h under N_2. At ~80 °C, Poly(**Y**) gradually changed to an orange polymer, Poly(**O**). Furthermore, Poly(**O**) gradually changed to a red colour polymer, Poly(**R**) when heated at 100 °C.

Measurements

The number and weight average molecular weights (M_n and M_w) of Poly(**Y**), Poly(**O**), and Poly(**R**) were measured using a JASCO GPC 900-1 equipped with two Shodex K-806L columns and an RI detector. Chloroform was used as an eluent at 40 ºC, and poly(styrene) standards (M_n = 800−1,090,000 Da) were employed for calibration. The

^{1}H and ^{13}C NMR spectra in solution were measured on a JEOL JNM-ECA500 in $CDCl_3$ at room temperature. Solid state ^{13}C CP-MAS NMR (125 MHz) spectra were measured on the same spectrometer using adamantine as a standard and 2 millisec as the contact time at room temperature. Diffuse reflective UV-vis spectra, DRUV-vis, of the polymers in the solid phase were recorded on a JASCO V570 spectrophotometer equipped with an ISV-470 integrating sphere accessory. Differential scanning calorimetry (DSC) was performed on a SHIMADZU DSC-60, and the traces were run in an atmosphere of N_2 at a heating rate of 10 °C/min. Wide-angle X-ray diffraction (XRD) patterns of the polymers were recorded on a RIGAKU RINT 2200 Ultima equipped with a heater and a PTC-30 programmable temperature controller. CuKα radiation was used as the X-ray source. The thermodynamically favoured conformation of the *p*OcPA 20-mer was determined by a molecular mechanics (MM) calculation using the MMFF 94 force field (Wavefunction, Inc., Spartan '10 Windows version 1.1.0).

Results and Discussion

Polymerisation

The polymerisations of *p*OcPA using the Rh complex catalyst and TEA cocatalyst in EtOH at -20 °C and 25 °C afforded Poly(**Y**) and Poly(**O**) in yields of 64 % and 99 %, respectively. Their number average molecular weights (M_n), polydispersities (M_w/M_n), and the *cis* percentages are listed in Table 1. The polymerisability of *p*OcPA was reduced at temperatures of less than -20 °C, and the *cis* ratio and the polydispersity were maintained. The *cis* % of the polymers was determined using ^{1}H NMR.[8,17] Previously, we reported that polar organic solvents such as EtOH and TEA induced the dissociation of the Rh catalyst into its catalytically active, solvent-stabilised monomeric species.[4] A bright orange polymer, Poly(**O**) with a *cis* ratio of 96 % was obtained in a yield of 99 % when the polymerisation was performed at 25 °C (Scheme 1 and Table 1). The *cis* % remained the same as that when the polymerisation was carried out at -20 °C. However, the M_n was fairly decreased from 37.1×10^4 to 26.9×10^4 at 25 °C compared to -20 °C.

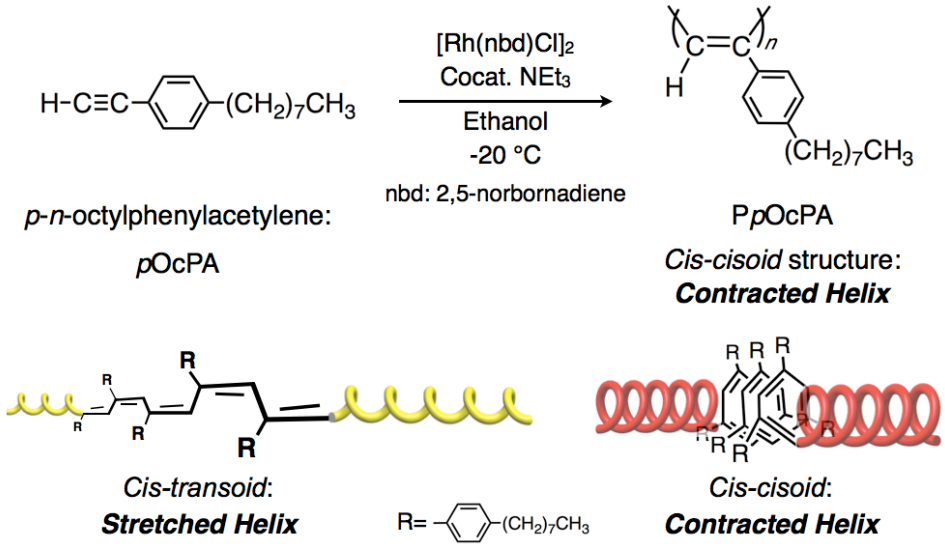

Scheme 1. Synthesis of poly(*p-n*-octylphenylacetylene) having ***contracted*** *cis-cisoid helices* using a $[Rh(nbd)Cl]_2$-TEA catalyst in EtOH at 25 °C.

This suggests that when the polymerisation is performed at 25 °C, the polymer decomposed and the M_n decreased. This is supported by the fact that the polydispersity increases from 2.0 at -20 °C to 4.4 at 25 °C. The decrease in molecular weight is attributed to the fairly stiff main chain, which is an important feature of *helical* π-conjugated polymers.

Table 1. Polymerisation of *p*OcPA with a $[Rh(nbd)Cl]_2$-NEt_3 catalyst[a]

Polymer	Solvent[b]	Polymn. temp. (°C)	Yield[d] (%)	M_n[e] $\times 10^{-4}$	M_w/M_n[e]	*Cis*[f] (%)	Colour
Poly(**Y**)	EtOH	-20	64	37.1	2.0	98	Yellow
Poly(**O**)	EtOH	25	99	26.9	4.4	96	Orange
Poly(**R**)	HT[c](EtOH)	-	-	23.4	3.2	90	Red

[a] Polymerisation conditions: 30 min, $[M]_0$ = 0.20 M, $[M]_0/[Rh\ cat.]$ = 100, $[NEt_3]/[Rh\ cat.]$ = 100. [b] Polymerization solvent used. [c] Prepared by heat treatment(HT) at 100 °C for 1 h under N_2 atmosphere. [d] MeOH insoluble part. [e] Estimated by GPC analysis (PSt, $CHCl_3$). [f] Determined by ^1H NMR analysis ($CDCl_3$).

Structural Characterisation by ^1H NMR

The ^1H NMR spectrum of Poly(**Y**) was measured in $CDCl_3$ at room temperature (Fig. 1) to determine its geometrical structure. The peaks observed at 6.67 and 6.51, 5.78, 2.36, 1.45, 1.25, and 0.88 ppm were assigned to the *meta* protons and the *ortho* protons in the phenyl rings; the vinyl protons in H^{α}-C=C; Ph-C^1H_2; C^2H_2; $(C^{3\sim7})H_{10}$; and C^8H_3 protons in the side alkyl chains, respectively. However, the ^1H NMR spectra of Poly(**O**) and Poly(**R**) were almost identical to the spectrum of Poly(**Y**). No significant difference in the chemical shifts, line shapes, or line widths among the polymers was detected in the solution phase, despite the large colour differences in the solid phase. Notably, the colours of the three polymers faded or were unchanged when the solid polymers were held at room temperature for a long time in the solid phase. Therefore, the colour

differences among Poly(**Y**), Poly(**O**), and Poly(**R**) were ascribed to morphological and/or conformational differences, such as the presence of *helical* structures, although SPAs in solution generally have been considered to have a *cis-transoid* structure called a ***Stretched*** *helix*^{CT}.[8(a)]

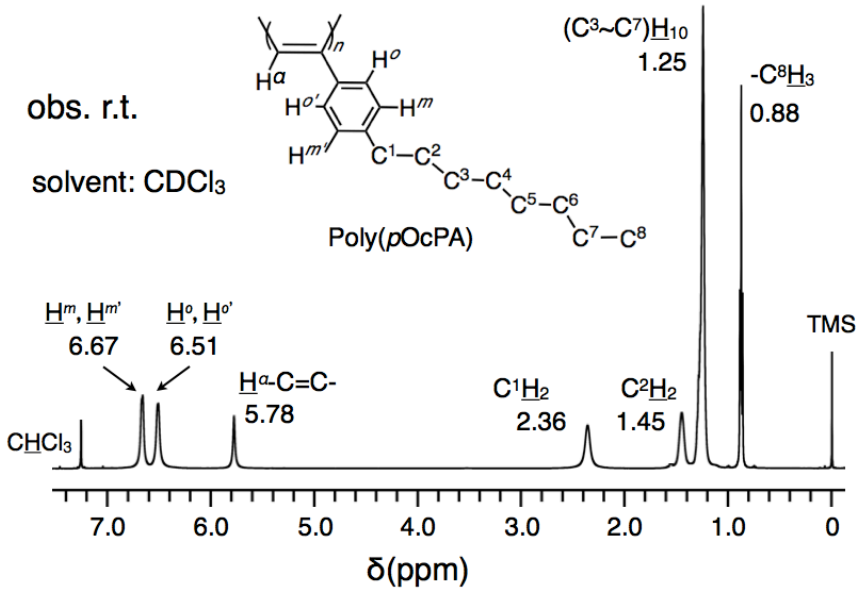

Figure 1. ^{1}H NMR spectrum of Poly(Y) observed at 25 °C in $CDCl_3$ solution.

Heat treatment of Poly(Y)

To determine the origin of the colour difference among the polymers, the pristine Poly(**Y**) powders were heated to 80 °C for 1 h using a test tube evacuated to 10^{-3} torr, and the *cis* ratio did not change (Table 1).[8a] While heating, Poly(**Y**) gradually changed to an orange polymer, Poly(**O**). Furthermore, the colour of Poly(**O**) changed to a red when heated to *ca.* 100 °C. Therefore, the origin of the colour difference in the solid

phase can be attributed to the morphological and/or conformational differences, including the presence of *helical* structures and/or crystal structure transitions.[8,20]

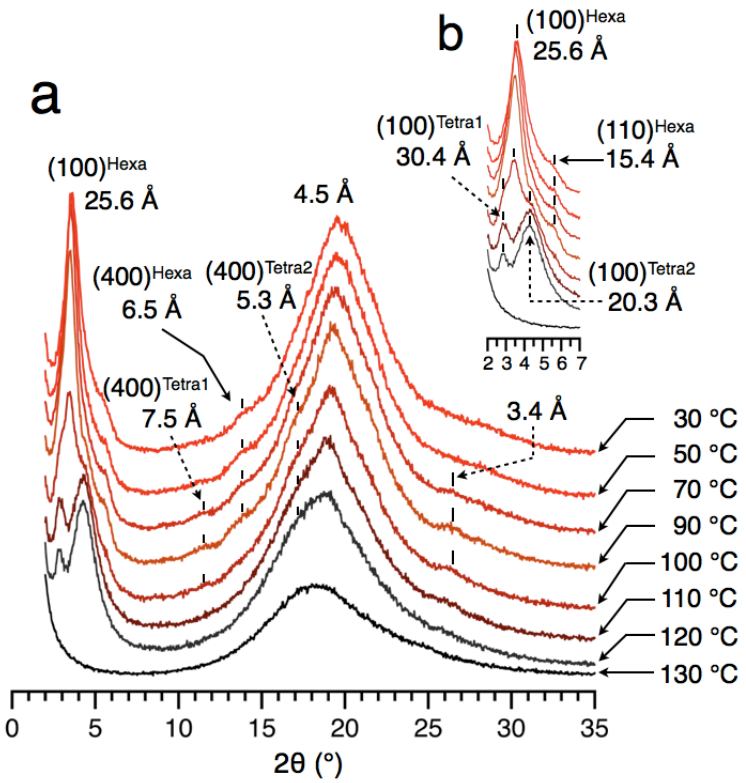

Figure 2. Temperature dependence of the XRD patterns of Poly(**Y**) measured from 30 °C to 130 °C under N_2 gas: (a) a full scale and (b) an expanded pattern from 2θ = 2° to 7°.

Crystal Structure Changes Detected by XRD

To explain the morphology and conformational differences, the XRD patterns of Poly(**Y**) were measured from 30 °C to 130 °C (Fig. 2). At 30 °C, two primary reflection peaks were observed: one at the low angle side, with a Bragg distance of d=25.6 Å, and

one at the higher angle side, with d=4.5 Å. This pattern was analysed under the assumption that the structure was a *hexagonal* columnar crystal with *contracted cis-cisoid helices* (=***contracted*** *helix*$^{\mathbf{CC}}$) (Fig. 3a). The peak at d=25.6 Å was attributed to the (100) reflection of the *hexagonal* columnar crystal. This assignment was supported by the appearance of peaks at 15.4 Å and 6.5 Å, which were attributed to the (110) and (400) reflections, respectively. In contrast to the ***stretched*** *cis-transoid helices* (=***stretched*** *helices*$^{\mathbf{CT}}$), were obtained *as the hexagonal* columnar crystals in the case of poly(*p*-*n*-hexoxyphenylacetylene) (P*p*HexOPA) prepared in EtOH at 25 °C.[8(a)] Therefore, the (100) reflection indicates that the column diameter, $D_{obs.}$, of the π-conjugated *helical* columnar was approximately 29.6 Å (=25.6/sin60°). The large broad peak at 4.5 Å was attributed to a halo peak superimposed with an intramolecular *n*-octyl alkyl chain distance in the side chain of Poly(**Y**), as previously reported.[8] The relatively small peak at d = 3.4 Å observed when heated to *ca.* 70-100 °C was attributed to the average intramolecular distance between the *helical* main chain rings and the neighbouring phenyl rings. These results indicate that the ***contracted*** *helix*$^{\mathbf{CC}}$ was stabilised in the solid phase. Additionally, these results also indicate that the intramolecular π-conjugation, i.e., π-stacking, occurred between neighbouring phenyl rings and/or the C=C alkene bonds of the *helical* backbone (Fig. 4). The Poly(**Y**) peak at d=25.6 Å gradually split into two reflection peaks at d=30.4 Å and 20.3 Å, respectively, when heated to *ca.* 100 °C. The half width of the peak at d=30.4 Å was small compared to the peak at d=20.3 Å. This difference clearly indicates that the two peaks arose from different crystal structures.

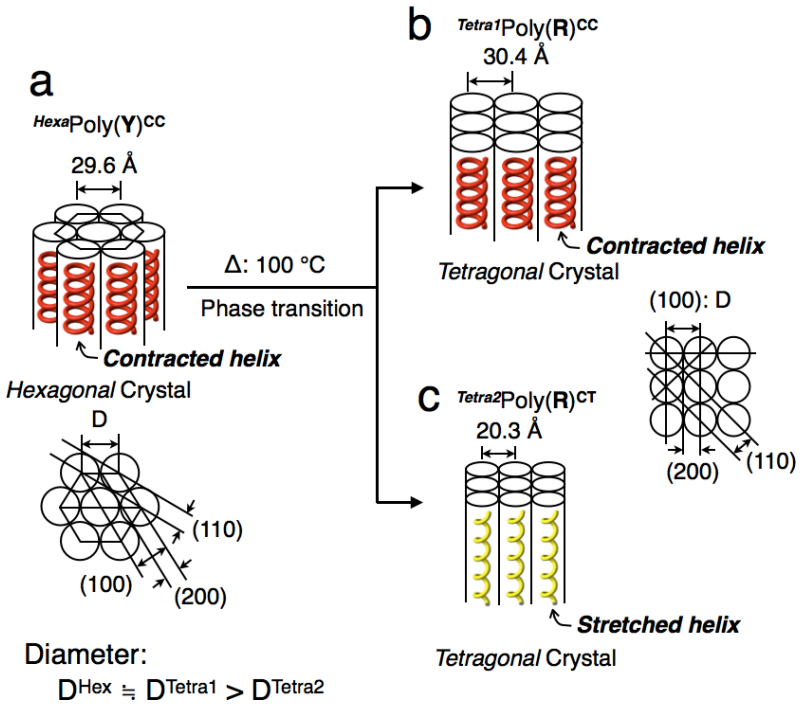

Figure 3. *Helix* to *Helix* rearrangement from (a) a *hexagonal* columnar crystal having ***contracted*** *cis-cisoid helices*, to (b) *tetragonal* crystal[1] having ***contracted*** *cis-cisoid helices,* and (c) *tetragonal* crystal[2] having ***stretched*** *cis-transoid helices*.

In other words, the peak at d=30.4 Å was attributed to a *tetragonal* crystal (***Tetra***^{1}) containing *cis-cisoid helices*, whereas the d=20.3 Å peak was attributed to an another *tetragonal* crystal (***Tetra***^{2}) containing *cis-transoid helices*, which are distinct from the pristine *hexagonal* columnar crystal structure (see Figs. 3a, b and c). Therefore, a solid phase transformation was corroborated to be surely induced by the heat treatment. The ***Tetra***^{1} peak at d=30.4 Å corresponded to an estimated *helical* diameter of 30.4 Å (Fig. 3b), and the ***Tetra***^{2} peak at 20.3 Å corresponded to an estimated *helical* diameter of 20.3 Å (Figs. 3c). The small peaks at 7.5 Å and 5.3 Å were also attributed to the (400) reflections of ^{Tetra1}Poly(**R**)^{CC} and ^{Tetra2}Poly(**R**)^{CT}, respectively. These peaks decayed at

approximately 130 °C, together with the π-stacking peak at 3.4 Å, as shown in Figs. 2a and b. This disappearance shows the melt of this polymer, as mentioned below. XRD patterns observed at approximately 80 °C agreed with the patterns of the Poly(**O**) that was prepared at 25 °C. This finding indicates that the polymerisation temperature is correlated to the resulting *helical* crystal and main chain structures. Therefore, these results allow us to conclude that Poly(**O**) and Poly(**R**) were composed from two *tetragonal* crystals in which two types of *helices*, the ***contracted*** *helix*$^{\mathbf{CC}}$ and ***stretched*** *helix*$^{\mathbf{CT}}$, are packed in the solid columnar phase. The thermal changes of the XRD patterns indicate that pristine $^{\textit{Hexa}}$Poly(**Y**)$^{\mathbf{CC}}$ is a thermodynamically unstable *helix* compared to $^{\textit{Tetra1}}$Poly(**R**)$^{\mathbf{CC}}$ and $^{\textit{Tetra2}}$Poly(**R**)$^{\mathbf{CT}}$.[21] Moreover, these findings were supported by the calculation of a model polymer, a 20-mer of *p*OcPA, using the MMFF 94 calculation method, as mentioned below. Thus, the diameter for $^{\textit{Hexa}}$Poly(**Y**)$^{\mathbf{CC}}$ is fairly fine with a magnitude of 9.3−10.1 Å compared to the ***contracted*** helices of $^{\textit{Tetra2}}$Poly(**R**)$^{\mathbf{CT}}$ and $^{\textit{Tetra1}}$Poly(**R**)$^{\mathbf{CC}}$. This allows us to conclude that $^{\textit{Hexa}}$Poly(**Y**)$^{\mathbf{CC}}$ is composed of ***contracted*** *helices* (Fig. 3).

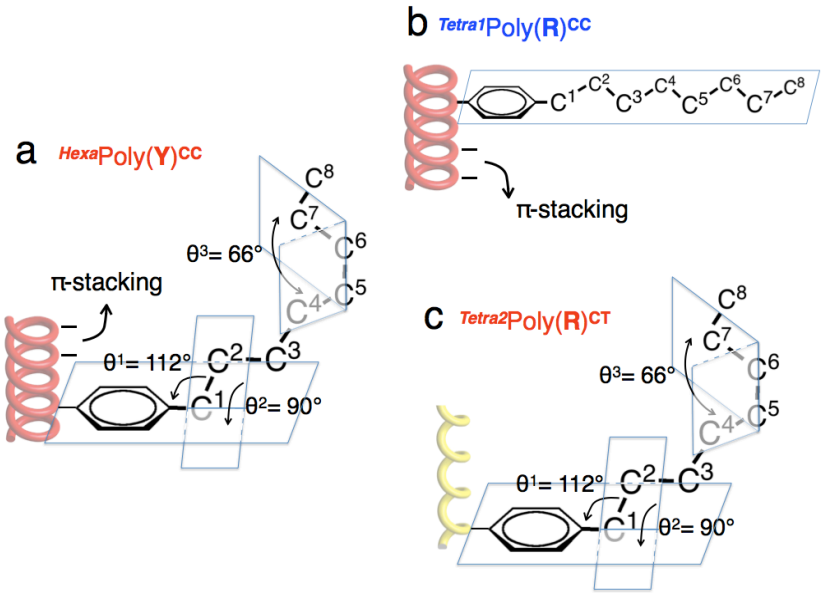

Figure 4. Calculated *helical* backbone, (a) a ***contracted*** *helix* with a bent *n*-octyl phenyl ring, (b) a ***contracted*** *helix* with an extended alkyl phenyl ring, and (c) a ***stretched*** *helix* with a bent *n*-octyl phenyl ring.

Energetically Stable Structures Calculated by MMFF 94

The most stable *helical* conformations of ^{Hexa}Poly(Y)^{CC}, ^{Tetra1}Poly(R)^{CC}, and ^{Tetra2}Poly(R)^{CT} were simulated using the *p*OcPA 20-mer as a model molecule. The molecular mechanics (MM) calculations used the MMFF 94 force field program.[8a] The MMFF 94 calculations were performed by rotating the dihedral angles, θ (°) along the centre C-C single bonds in the C=C-C=C moieties. These calculations were assumed that the alkyl chains have a bent structure at the C^6 carbon in ^{Hexa}Poly(Y)^{CC} (see Fig. 4a), an extended alkyl chain in ^{Tetra1}Poly(R)^{CC} (Fig. 4b), and the same bent structure in ^{Tetra2}Poly(R)^{CT}(Fig. 4c). Moreover, the bent angles, θ, between the benzene ring and the alkyl chain were assumed to take θ^1=112° and θ^2=90°, respectively, and the bond angle

between the C^4-C^5 and C^6-C^7 carbons was also assumed to be approximately θ^3=66°. Thus, the stable conformation of the alkyl benzene ring was optimised in advance using the MMFF 94 program. These calculations afforded the relationship between θ and the strain energy (kJ/unit mol) (Fig. 6). These results clearly demonstrated that the strain energy was minimised, (122.5 kJ/unit mol) at approximately θ=110° in the case of the extended alkyl chain (see Fig. 4c). This indicated that the model polymer having such a bent alkyl chain can exist as two stable conformations at θ=70° and 110°, respectively (see Fig. 6). When the dihedral angle is 70°, the *contracted* and *stretched* helices take bent alkyl chain and *zig-zag* straight chain, respectively. Therefore, the final conformations between the two *contracted* helices having the bent alkyl chain and the straight alkyl chain are different each other, irrespective of the same dihedral angles. In other words, the dihedral angles in ^{Hexa}Poly(**Y**)^{CC} and ^{Tetra2}Poly(**R**)^{CT} take θ=70° and 110°, respectively, and have *contracted cis-cisoid* and *stretched cis-transoid helices*, respectively. Thereby, the diameters of ^{Hexa}Poly(**Y**)^{CC} and ^{Tetra2}Poly(**R**)^{CT} were determined to be $D_{calc.}$=29.6 Å and 20.4 Å, respectively, which are in agreement with the diameters obtained by XRD, $D_{obs.}$=29.6 Å and 20.3 Å. On the other hand, in the case of the *helical* main chain having such an extended alkyl chain the minimum energy reached to *ca.* 114.5 kJ/unit mol at θ=70°. This indicates that ^{Tetra1}Poly(**R**)^{CC} has a calculated diameter of $D_{calc.}$=30.8 Å, while the diameter determined by XRD is $D_{obs.}$=30.4 Å (see Figs. 3b and 5b). Thus, the MMFF 94 calculations agreed with the determined diameters, indicating high calculation reliability.

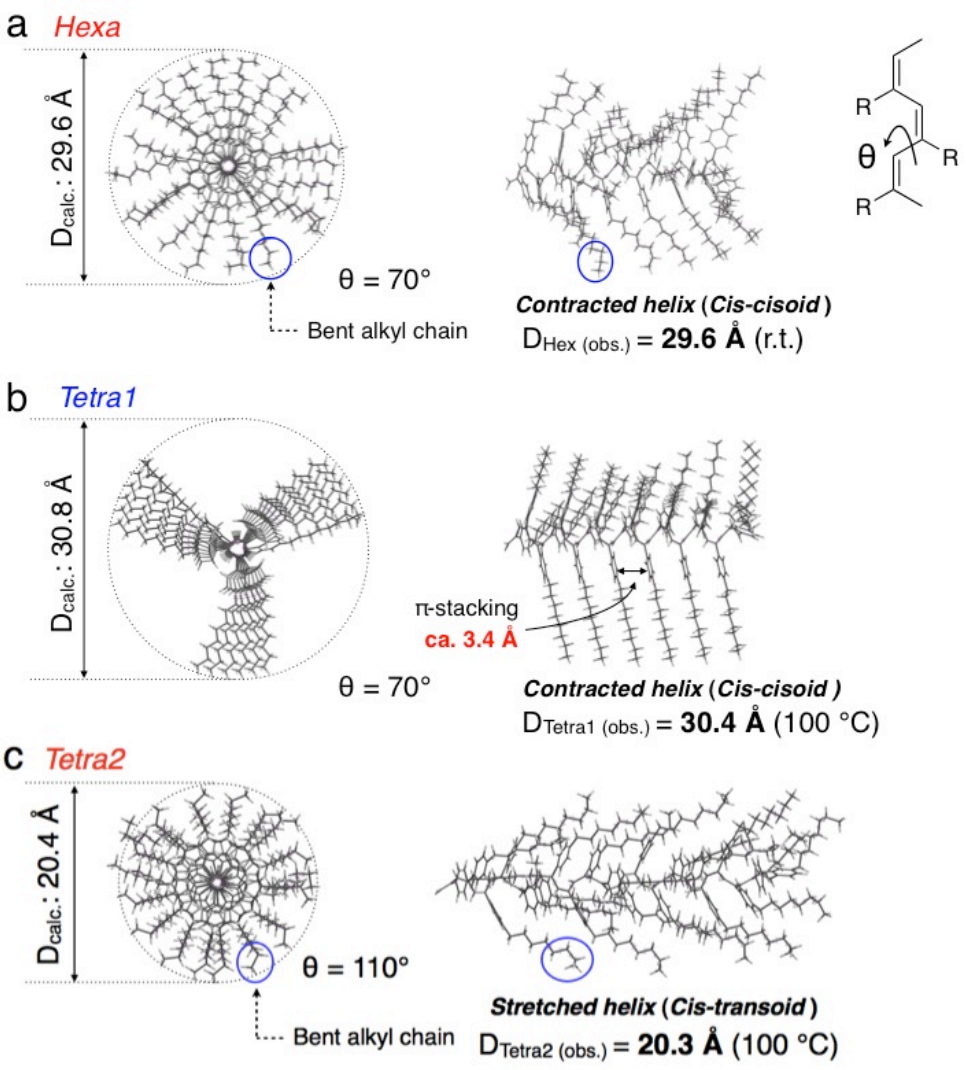

Figure 5. Observed and calculated *helix* diameters of Poly(**Y**) obtained before and after heat treatment at 100 °C for 1 h: (a) a *hexagonal* columnar crystal having ***contracted*** *cis-cisoid helices*, (b) a *tetragonal* crystal having ***contracted*** *cis-cisoid helices*, (c) a *tetragonal* crystal having ***stretched*** *cis-transoid helices*.

Furthermore, the calculations for the model polymer of ^{Tetra1}Poly(**R**)^{CC} indicate that the distances between every *helical* pitch width, i.e., p-stacking of the phenyl rings with extended alkyl chains is approximately 3.4 Å, which was observed at approximately

70-100 °C in the XRD patterns. Thus, the calculated *helical* pitch width agrees well with the observed *helical* pitch. However, notably the possibility regarding formation of rectangular crystal instead of the two *tetragonal* crystals is not always excluded as reported by Percec et al.[14d]

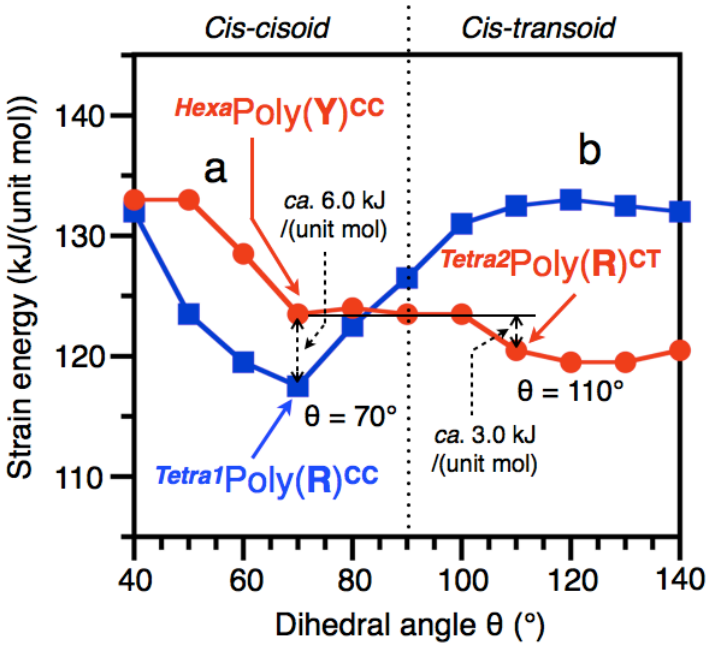

Figure 6. Strain energy dependences of dihedral angles θ° around the C-C single bond in the C=C-C=C bond in (a) an extended alkyl chain and (b) a bent alkyl chain.

π-Conjugation Length in the Solid Phase

The DRUV-vis spectra of Poly(Y), Poly(O), and Poly(R) are shown in Fig. 7. The absorption maximum, λ_{max}, of Poly(Y) was observed at 448 nm with a shoulder at 565 nm. The absorption at 448 nm was attributed to *contracted cis-cisoid helices* in ^{Hexa}Poly(Y)^{CC}.[8(a)]

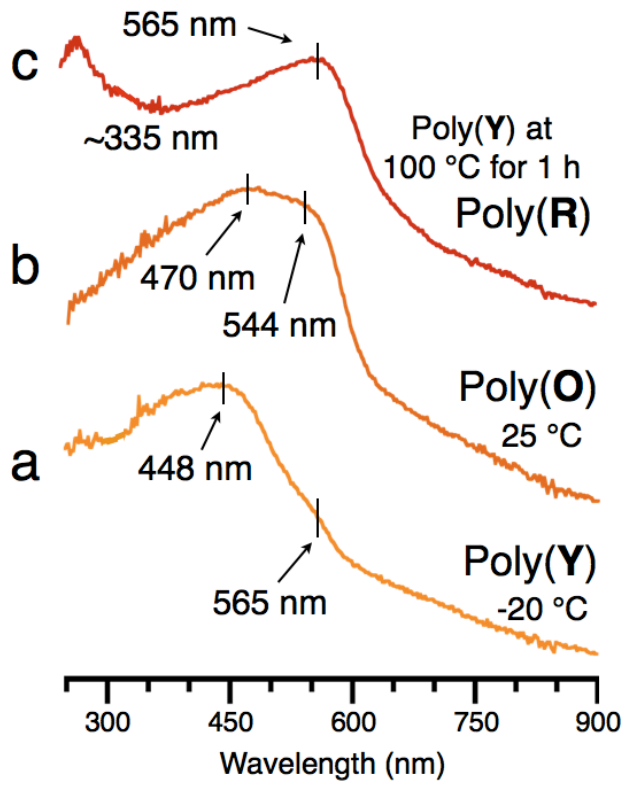

Figure 7. DRUV-vis spectra of (a) Poly(**Y**), (b) Poly(**O**), and (c) Poly(**R**) observed on alumina powders.

Previously, *cis* and *trans* polyacetylenes with no substituents prepared using the Ziegler-Natta catalyst Et_3Al-Ti(O*n*-Bu)$_4$ showed λ_{max} at 570 and 675 nm with small shoulders at approximately 500 and 600 nm, respectively.[22] The λ_{max} at 448 nm in ^{Hexa}Poly(Y)^{CC} shifted to 565 nm when heated to 100 °C for 1 h. This observation indicated that the *helical* pitch was shortened to accommodate ordered π-stacking along the helical backbone. Therefore, the λ_{max} at 565 nm was attributed to the ^{Tetra1}Poly(R)^{CC}, although the absorption of ^{Tetra2}Poly(R)^{CT} is superimposed on this peak to some extent. The DRUV-vis spectrum of Poly(**O**) was attributed to be an intermediate between the spectra of Poly(**Y**) and Poly(**R**).

Bent *n*-Octyl Alkyl Chains Detected by Solid State ^{13}C CP-MAS NMR

Solid state ^{13}C CP-MAS NMR was used to determine whether the *n*-octyl side chains of ^{Hexa}Poly(Y)^{CC} and ^{Tetra2}Poly(R)^{CT} hold a linear or a bent structure in the solid phase, in addition to the position of the bend. Because the XRD data and MMFF 94 calculations indicated that the two polymers have a bent alkyl chain (see Figs. 4a, c, 5a, and c).

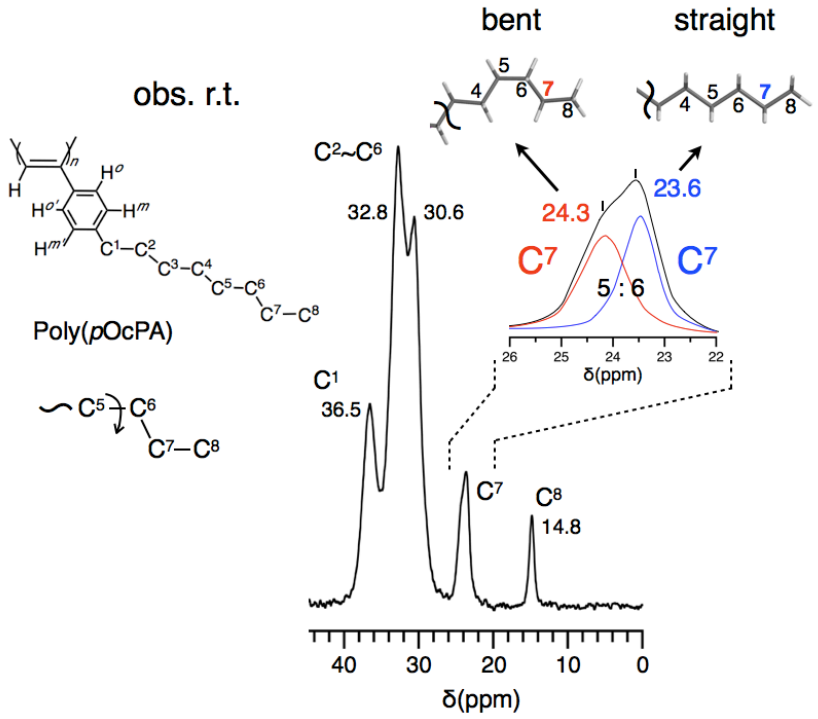

Figure 8. Solid state ^{13}C CP-MAS NMR spectra from 0 to 45 ppm of Poly(**Y**) at room temperature.

Fig. 8 shows only the alkyl carbon chemical shift region from 0 to 45 ppm. The peaks at 36.5, 32.8, 30.6, 24.3, 23.6, and 14.8 ppm were attributed to the C^1H_2, $C^{2\sim6}H_2$, C^7H_2, $C^{7'}H_2$, and C^8H_3 carbons, respectively. This assignment was confirmed by the solution

^{13}C NMR spectrum (see Figs. S1 and S2).† Interestingly, the peak due to C^7 at the second position from the terminal methyl moiety was found to be splitted into two peaks at 23.6 and 24.3 ppm, respectively, having a ratio of 5:6 (Fig. 8). It is necessary to note that the intensity of the ^{13}C peaks is not related to the formation ratio of the extended and bent carbon chains but is related to the contact time used. The peaks at 23.6 and 24.3 ppm were assigned to the normal *zigzag* extended C^7 methylene carbons and the bent carbons at C^7, respectively,[23] although the position of the bend is at the C^6 carbon. Thus, we corroborated that the bend position within the alkyl chain structure is at the C^6 carbon using the solid state ^{13}C CP-MAS NMR method, although such a bent alkyl chain structure in the columnar has never been reported to the best of our knowledge.

DSC Studies

Fig. 9 shows the DSC trace of Poly(Y) measured under nitrogen from 50 to 180 °C at a heating rate of 10 °C/min. The trace exhibited three endothermic peaks at approximately 82, 105, and 145 °C, respectively. The second peak at *ca.* 105 °C was attributed to the solid phase transition from the *hexagonal* structure having the *contracted helix*^{CC} with *cis-cisoid helices* to the *tetragonal* crystal, *Tetra*^{1}, with *contracted cis-cisoid helices* and tetragonal crystals, *Tetra*^{2}, with *stretched helices*^{CT}. The small endotherm at ca. 82°C was attributed to the melt or reorientation of the *n*-octyl alkyl side chains. Such small reorientation peaks are often observed before a phase transition.[24] Notably, the thermal treatment of Poly(Y) under N_2 for 1 h at a

temperature greater than 140 °C rapidly decreased the *cis* % because of the *cis*-to-*trans* isomerisation as evidenced by the DSC trace.[8(a)] The enthalpy of the transition energy (ΔH_2= *ca.* 0.61 kJ/unit mol) corresponded to the thermally induced rearrangement of ^{Hexa}Poly(Y)^{CC} to ^{Tetra1}Poly(R)^{CC} and ^{Tetra2}Poly(R)^{CT}. This enthalpy value was approximately 1/10 of the calculated transition energy (6.0 kJ/unit mol) obtained from the MMFF 94 method (Fig. 6). This inconsistency was rationalised in terms of columnar structure. Because both the rotational angles around the primary alkyl chain and the position of the long alkyl chain require to be changed during the solid phase transition of ^{Hexa}Poly(Y)^{CC} to ^{Tetra1}Poly(R)^{CC} and ^{Tetra2}Poly(R)^{CT}. Therefore, the thermally induced rearrangement did not proceed to completion. In other words, less than 1/10 of the *helical* components in ^{Hexa}Poly(Y)^{CC} rearrange to ^{Tetra1}Poly(R)^{CC} and ^{Tetra2}Poly(R)^{CT} in the solid phase. Furthermore, it is noteworthy that the thermal treatment of ^{Hexa}Poly(Y)^{CC} at *ca.* 100 °C did not appreciably decrease the *cis* %. This indicates that the *cis*-to-*trans* isomerisation reaction was not significantly induced even during this heat treatment in the solid phase. This also suggests that half of the Poly(O) remains unchanged when heated to 80 °C. Consequently, the boundary sequences between the unchanged Poly(O) and the changed Poly(R) are relatively short and produce distorted sequences. This distortion is the reason why a small absorption at ~320 nm is created when heated to 100 °C, as shown in Fig. 9.

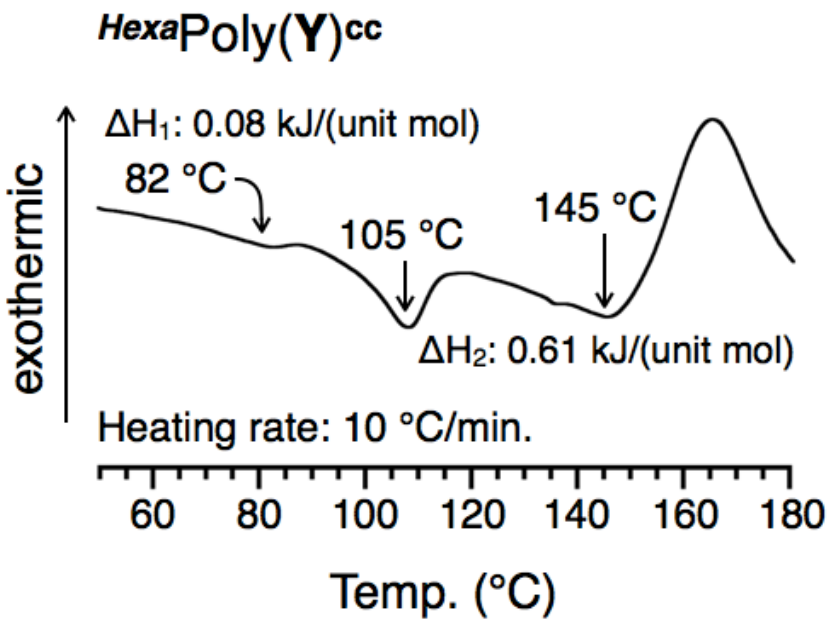

Figure 9. DSC thermogram of Poly(Y) observed from 50 to 180 °C.

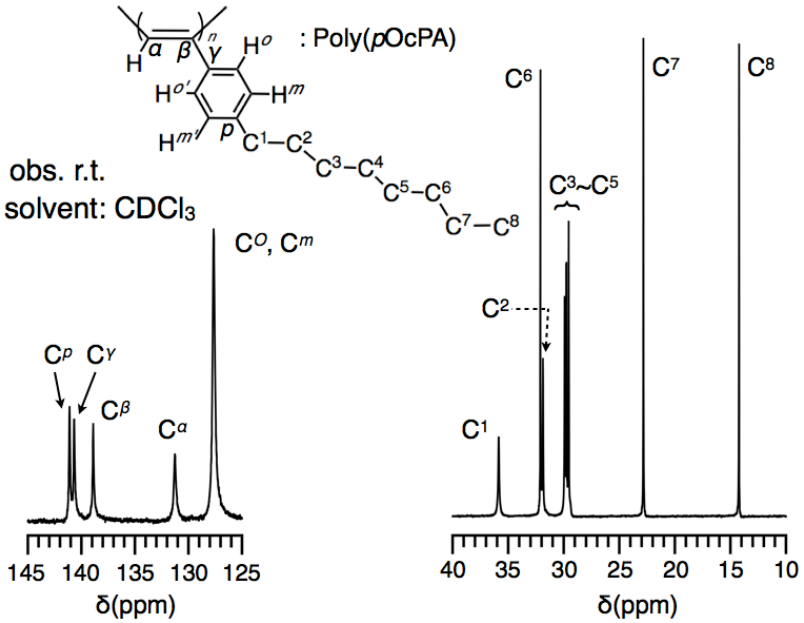

Fig. S1 ^{13}C NMR spectrum of poly(*p*-*n*-octyphenylacetylene) observed at 25 °C in $CDCl_3$ solution.

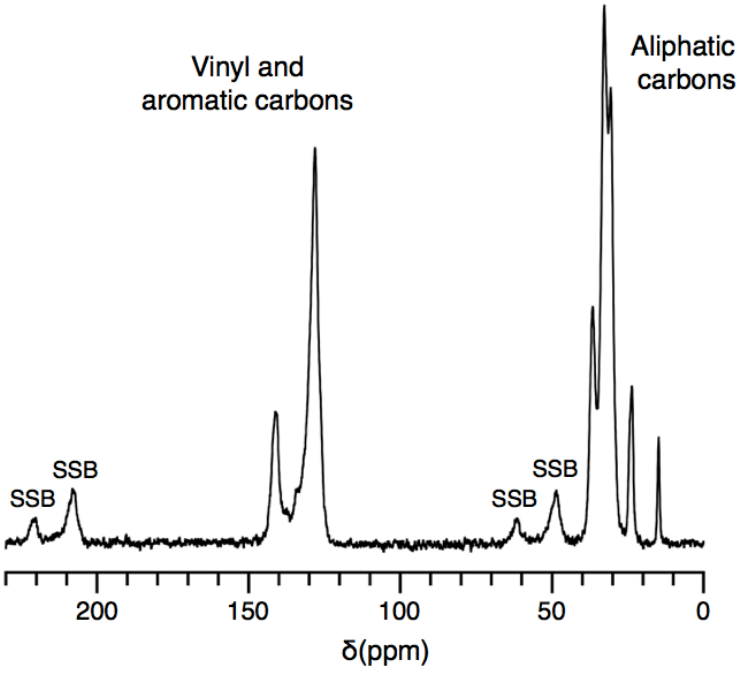

Fig. S2 Solid state ^{13}C CP-MAS NMR spectra of Poly(**Y**) at room temperature.

Conclusions

p-*n*-Octylphenyacetylene (*p*OcPA) was stereoregularly polymerised at -20 °C and 25 °C using $[Rh(nbd)Cl]_2$ and a TEA cocatalyst in EtOH to afford yellow and orange polymers, Poly(**Y**) and Poly(**O**), in high yields of 64 and 99 %, respectively. Poly(**Y**) transformed into red polymer, Poly(**R**), upon heating to 100 °C. The three polymers were analysed by XRD, MMFF 94 calculations, DSC, DRUV-vis, and solid state ^{13}C CP-MAS NMR. Poly(**Y**) and Poly(**R**) exhibited absorption maximums, λ_{max}, at 448 and 565 nm, respectively. No significant differences were observed in the ^{1}H NMR spectra obtained in chloroform. The XRD patterns of Poly(**Y**) revealed that it has a *hexagonal* columnar crystal structure comprising *cis-cisoid helices*, i.e., ***contracted*** *helices*, called

^{Hexa}Poly(**Y**)^{CC}. Furthermore, heating ^{Hexa}Poly(**Y**)^{CC} up to 100 °C induced a solid phase transformation to the red polymers, ^{Tetra1}Poly(**R**)^{CC} and ^{Tetra2}Poly(**R**)^{CT}. The XRD pattern of Poly(**O**) agreed with the pattern of Poly(**Y**) that was heated to *ca.* 90 °C. To the best of our knowledge, such solid phase rearrangements resulting from a ***contracted*** *helix*^{CC} to a ***stretched*** *helix*^{CT} accompanied by a drastic colour change have never been reported. The thermal instability of ^{Hexa}Poly(**Y**)^{CC} was proven by the DSC endotherm at *ca.* 105 °C. Moreover, the XRD and MMFF 94 data of the *n*-octyl chains of ^{Hexa}Poly(**Y**)^{CC} and ^{Tetra2}Poly(**R**)^{CT} showed that the octyl side chain in the phenyl rings bend at the third carbon from the terminal methyl group, i.e., C^6. Therefore, these data clearly corroborated that ^{Hexa}Poly(**Y**)^{CC} crystals are thermally converted to the two *tetragonal* crystals containing ***contracted*** *helices*^{CC} and ***stretched*** *helices*^{CT} at 100 °C.

Reference

1. R. J. Kern, *J. Polym. Sci.: Polym. Chem. Ed.* **1969**, 7, 621-631.
2. L. B. Luttinger, *J. Org. Chem.* **1962**, 27, 1591-1596.
3. T. Masuda and T. Higashimura, *Adv. Polym. Sci.* **1986**, 81, 121-165.
4. (*a*) M. Tabata, W. Yang, K. Yokota, *Polym. J.* **1990**, 22, 1105-1107. (*b*) W. Yang, M. Tabata, K. Yokota, *Polym. J.* **1991**, 23, 1135-1138. (*c*) M. Tabata, W. Yang, K. Yokota, *J. Polym. Sci. Part A: Polym. Chem.* **1994**, 32, 1113-1120. (*d*) M. Lindgren, H. S. Lee, W. Yang, M. Tabata, K. Yokota, *Polymer* **1991**, 32, 1532–1534. (*e*) Y. Yoshida, Y. Mawatari, C. Seki, T. Hiraoki, H. Matsuyama, M. Tabata,

Polymer **2011**, 52, 646-651. (f) B. Z. Tang, X. Kong, X. Wan, *Macromolecules* **1997**, 30, 5620-5628.(g) T. Aoki, T. Kaneko, N. Maruyama, A. Sumi, M. Takahashi, T. Sato, M. Teraguchi, *J. Am. Chem. Soc.* **2003**, 125, 6346-6347. (h) A. Nakazato, I. Saeed, T. Katsumata, M. Shiotsuki, T. Masuda, J. Zednik, J. Vohlidal, *J. Polym. Sci. Part A: Polym. Chem.* **2005**, 43, 4530–4536. (i) I. Saeed, M. Shiotsuki, T. Masuda, *Macromolecules* **2006**, 39, 5347-5351.

5. (*a*) Y. Kishimoto, P. Eckerle, T. Miyataka, M. Kainosho, A. Ono, T. Ikariya, R. Noyori, *J. Am. Chem. Soc.* **1999**, 121, 12035-12044. (*b*) N. Onishi, M. Shiotsuki, F. Sanda, T. Masuda, *Macromolecules* **2009**, 42, 4071-4076. (*c*) T. Nishimura, Y. Ichikawa, T. Hayashi, N. Onishi, M. Shiotsuki, T. Masuda, *Organometallics* **2009**, 28, 4890-4893. (*d*) M. Shiotsuki, N. Onishi, F. Sanda, T. Masuda, *Chem. Lett.* **2010**, 39, 244-245. (*e*) M. Shiotsuki, F. Sanda, T. Masuda, *Polym. Chem.* **2011**, 2, 1044-1058.

6. (*a*) M. Tabata, Y. Inaba, K. Yokota, Y. Nozaki, *J. Macromol. Sci. Pure Appl. Chem.* **1994**, A31, 465-475. (*b*) M. Tabata, Y. Sadahiro, Y. Nozaki, Y. Inaba, K. Yokota, *Macromolecules* **1996**, 29, 6673-6675. (*c*) M. Tabata, S. Kobayashi, Y. Sadahiro, Y. Nozaki, K. Yokota, W. Yang, *J. Macromol. Sci. Pure Appl. Chem.* **1997**, A34, 641–653.

7. G. Unger, *Polymer* **1993**, 34, 2050-2059.

8. (*a*) A. Motoshige, Y. Mawatari, Y. Yoshida, C. Seki, H. Matsuyama, M. Tabata, *J. Polym. Sci. Part A: Polym. Chem.* **2012**, 50, 3008–3015. (*b*) Y. Mawatari, M. Tabata, *J. Jpn. Soc. Colour Mater.* **2009**, 82, 204–209. (*c*) Y. Mawatari, M. Tabata,

T. Sone, K. Ito, Y. Sadahiro, *Macromolecules* **2001**, 34, 3776–3782.

9. (*a*) T. Masuda, E. Isobe, T. Higashimura, K. Takada, *J. Am. Chem. Soc.* **1983**, 105, 7473-7474. (*b*) T. Masuda, K. Nagai, in *Materials Science of Membranes*, ed. Y. Yampolskii, I. Pinnau and B. D. Freeman, Wiley, Chichester, UK, **2006**, ch. 8.

10. (*a*) D. Neher, A. Wolf, C. Bubeck, G. Wegner, *Chem. Phys. Lett.* **1989**, 163, 116-122. (*b*) J. L. Bredas, C. Adant. P. Tacks, A. Persoons, M. Pierce, *Chem. Rev.* **1994**, 94, 243-278. (*c*) M. Falconieri, R. D'Amato, M. V. Russo, A. Furlani, *Nonlinear Opt.* **2001**, 27, 439-442. (*d*) M. Tabata, T. Sone, K. Yokota, T. Wada, H. Sasabe, *Nonlinear Opt.* **1999**, 22, 341-344. (*e*) T. Wada, L. Wang, H. Okawa, T. Masuda, M. Tabata, M. Wan, M. Kakimoto, Y. Imai, H. Sasabe, *Mol. Cryst. Liq. Cryst.* **1997**, 294, 245-250.

11. (a) *Handbook of Conducting Polymers*, ed. T. A. Skotheim, Dekker, New York, **1986**, vol. 1–2. (b) *Introduction to Synthetic. Electrical Conductors*, ed. J. R. Ferraro and J. M. Williams, Academic Press Inc, New York, **1987**. (c) *Polymeric. Materials*, ed. J. C. Salomone, CRC Press, New York, **1996**, vol. 8.

12. (*a*) Y. V. Korshak, T. V. Medvedeva, A. A. Ovchinnikov, V. Spector, *Nature* **1987**, 326, 370-372. (*b*) N. Tyutyulkov, K. Müllen, M. Baumgarten, A. Ivanova, A. Tadjer, *Synth. Met.* **2003**, 139, 99-107. (*c*) M. Tabata, Y. Nozaki, W. Yang, K. Yokota, Y. Tazuke, *Proc. Jpn. Acad.* **1995**, 71, 219-224. (*d*) *Spin glass*, K. H. Fisher, J. A. Herz, Cambridge University Press, Cambridge, **1991**. (*e*) J. J. Pregjean and J. Souletie, *J. Phys.*, **1980**, 41, 1335-1352. (*f*) L. Floch, F. Hammann, J. Ocio, M. Vincent, *Euro. Phys. Lett.* **1992**, 18, 647-652. (*g*) D. G. Xenikos, H.

Multer, C. Jouan, A. Suilpice, J. L. Tholence, *Solid State Commun.* **1997**, 102, 681-685. (*h*) M. Tabata, Y. Watanabe, S. Muto, *Macromol. Chem. Phys.* **2004**, 205, 1174-1178. (*i*) Y. Watanabe, S. Muto, M. Tabata, *Jpn. J. Appl. Phys. Part 2 Lett.* **2004**, 43, 300-302.

13. (*a*) R. J. M. Nolte, *Chem. Soc. Rev.* **1994**, 23, 11−19. (*b*) J. J. L. M. Cornelissen, A. E. Rowan, R. J. M. Nolte, N. A. J. M. Sommerdijk, *Chem. Rev.* **2001**, 101, 4039−4070. (*c*) Y. Ito, T. Miyake, S. Hatano, R. Shima, T. Ohara, M. Suginome, *J. Am. Chem. Soc.* **1998**, 120, 11880−11893. (*d*) T. Nakano, Y. Okamoto, *Chem. Rev.* **2001**, 101, 4013−4038. (*e*) O. Vogl, *CHEMTECH* **1986**, 698−703. (*f*) K. Ariga, T. Kunitake, *Acc. Chem. Res.* **1998**, 31, 371−378. (*g*) A. Abe, Y. Imada, H. Furuya, *Polymer* **2010**, 51, 6234−6239.

14. (*a*) Y. K. Kwon, S. N. Chvalun, J. Blackwell, V. Percec, J. A. Heck, *Macromolecules* **1995**, 28, 1552-1558. (*b*) K. Maeda, E. Yashima, *J. Syn. Org. Chem. Jpn.* **2002**, 60, 878−890. (*c*) V. Percec, G. J. Rudick, M. Peterca, M, Wagnar, M. Obata, M. C. Mitchell, W. Cho, S. K. V. Balagurusamy, A. P. Heiney, *J. Am. Chem. Soc.* **2005**, 127, 15257-15264. (*d*) V. Percec, J. G. Rudick, M. Peterca, E. Aqad, M. R. Imam, P. A. Heiney, *J. Polym. Sci. Part A: Polym. Chem.* **2007**, 45, 4974-4987. (*e*) V. Percec, G. J. Rudick, M. Peterca, A. P. Heiney, *J. Am. Chem. Soc.* **2008**, 130, 7503-7508. (*f*) K. P. Liu, Z. Q. Yu, J. H. Liu, E. Q. Chen *Macromol. Chem. Phys.* **2009**, 210, 707-716.

15. (*a*) F. Sanda, T. Masuda, *J. Synth. Org. Chem., Jpn.* **2008**, 66, 757–764. (*b*) M. Shiotsuki, F. Sanda, T. Masuda, *Polym. Chem.* **2011**, 2, 1044–1058. (*c*) T. Aoki, T.

Kaneko, M. Teraguchi, *Polymer* **2006**, 47, 4867–4892.

16. (*a*) E. Yashima, T. Matsushima, Y. Okamoto, *J. Am. Chem. Soc.* **1995**, 117, 11596–11597. (*b*) K. Maeda, H. Goto, E. Yashima, *Macromolecules* **2001**, 34, 1160–1164. (*c*) R. Nomura, Y. Fukushima, H. Nakako, T. Masuda, *J. Am. Chem. Soc.* **2000**, 122, 8830–8836. (*d*) R. Nomura, H. Nakako, T. Masuda, *J. Mol. Catal A: Chem.* **2002**, 190, 197–205. (*e*) E. Yashima, K. Maeda, H. Iida, Y. Furusho, K. Nagai, *Chem. Rev.* **2009**, 109, 6102–6211.
17. (*a*) M. Tabata, T. Sone, Y. Sadahiro, *Macromol. Chem. Phys.*, **1999**, 200, 265–282. (*b*) M. Tabata, Y. Sadahiro, T. Sone, K. Yokota, Y. Ishikawa, *J. Polym. Sci. Part A: Polym. Chem.* **1998**, 36, 2457-2461. (*c*) K. Huang, Y. Mawatari, A. Miyasaka, Y. Sadahiro, M. Tabata, Y. Kashiwaya, *Polymer* **2007**, 48, 6366-6373. (*d*) T. Sone, R. Asako, T. Masuda, M. Tabata, T. Wada, H. Sasabe, *Macromolecules* **2001**, 34, 1586-1592. (*e*) T. Sone, R. Amato, Y. Mawatari, M. Tabata, A. Furlanl, M. V. Russo, *J. Polym. Sci. Part A: Polym. Chem.* **2004**, 42, 2365-2376.
18. (*a*) Y. Yoshida, Y. Mawatari, A. Motoshige, R. Motoshige, T. Hiraoki, M. Wagner, K. Müllen, M. Tabata, *J. Am. Chem. Soc.* **2013**, 135, 4110-4116. (*b*) Y. Yoshida, Y. Mawatari, A. Motoshige, R. Motoshige, T. Hiraoki, M. Tabata, *Polym. Chem.* **2013**, 4, 2982-2988.
19. S. Ito, M. Wehmeier, J. Brand, C. Kübel, R. Epsch, J. Rabe, K. Müllen, *Chem. Eur. J.* **2000**, 6, 4327-4342.
20. (*a*) K. Huang, M. Tabata, Y. Mawatari, A. Miyasaka, E. Sato, Y. Sadahiro, Y. Kashiwaya, K. Ishii, *J. Polym. Sci. Part A: Polym. Chem.* **2005**, 43, 2836-2850. (*b*)

M. Tabata, Y. Mawatari, T. Sone, A. Miyasaka, K. Huang, K. Orito, Y. Sadahiro, *Macromol. Symp.* **2006**, 239, 7-12.

21. A. Motoshige, Y. Mawatari, R. Motoshige, Y. Yoshida, M. Tabata, *J. Polym. Sci. Part A: Polym. Chem.* **2013**, 51, 5177-5183.
22. I. Harada, M. Tasumi, H. Shirakawa S. Ikeda, *Chem. Lett.*, **1978**, 1441.
23. *Spectrometric Identification of Organic Compounds*, R. M. Silverstein, F. X. Webster, D. J. Kiemle, John Wiley & Sons. Inc, New York, **2005**.
24. B. Ewen, G. R. Strobl, D. Richter, *Faraday Discuss. Chem. Soc.* **1980**, 69, 19-31.

Summary of this Thesis

The polymerization of *p*-*n*-alkoxyphenylacetylene and *p*-*n*-alkylphenylacetylene was carried out by using a [Rh(norbornadine)Cl]$_2$-triethylamine catalyst to afford stereoregular helical poly(*p*-*n*-alkoxyphenylacetylene)s and poly(*p*-*n*-alkylphenylacetylene)s in the presence of solvent. We could show that the helical polyacetylenes have stretched helix, *cis-transoid* main-chain structure and *cis-cisoid* main-chain structure, contracted helix, respectively. Futhermore, we found that their polymer colors are related to the geometric structures and/or higher-order structures of the resulting polymers in solid phase. The helical pitches and colors of their polymers were changed by the heat-treatment accompanied with the transformation of the crystal structures in solid phase.

Chapter 1, The stereospecific polymerization of *p*-*n*-hexyloxyphenyacetylene was successfully performed using a [Rh(norbornadine)Cl]$_2$-triethylamine catalyst in ethanol or hexane at 25 °C to afford poly(**Y**) with a bright yellow color and poly(**R**) with a purple red color as powders, selectively, in fairly high yields. The XRD patterns of poly(**Y**) showed columnar structures comprising of the helical chains for both polymers, and the pitch of poly(**R**) is narrower than that of poly(**Y**). Interestingly a thermally induced rearrangement from the yellow poly(**Y**) to a reddish black polymer, poly(**Y→B**) took place at 80 °C. Poly(**Y→B**) showed that the helix diameter is near to poly(**R**). This means that poly(**Y**) is thermodynamically less stable helix compared to that of poly(**R**). The thermal instability of poly(**Y**) was proven by the fact that its exothermic transition temperature was observed at 80 °C. Thus, these data clearly

indicated that the *stretched helix* polymer, poly(**Y**), was changed to the *contracted helix* polymer, poly(**Y→B**), when heated at 80 °C under N_2.

Chapter 2, *p*-*n*-heptylphenylacetylene was stereoregularly polymerized using [Rh(norbornadiene)Cl]$_2$ and triethylamine in *n*-hexane, to afford the purple-red polymer Poly(**R**) in high yield. Poly(**R**) transformed into the black polymer Poly(**B**) upon heating to 80 °C. The XRD patterns of Poly(**R**) revealed that it had a hexagonal crystal structure (^{Hexa}Poly(**R**)) comprising *cis-cisoid helices* (*i.e., contracted helices* called ^{Hexa}Poly(**R**)^{CC}). Furthermore, heating Poly(**R**) up to 120 °C induced the solid phase transformation of ^{Hexa}Poly(**R**)^{CC} to two tetragonal crystal phases: one containing large-diameter *cis-cisoid helices* and the other containing small-diameter *stretched helices*. The thermal instability of ^{Hexa}Poly(**R**)^{CC} was proven by the DSC endotherm at approximately 80 °C. These data clearly corroborated that the pristine ^{Hexa}Poly(**R**)^{CC} crystals thermally converted into the two tetragonal crystals containing *contracted helices*^{CC} and stretched *helices*^{CT} at approximately 80 °C, respectively. The origin of the color changes observed before and after the heat treatment was attributed to the helical pitch width and the increment of intramolecular π-stack order in the polymer chain.

Chapter 3, *Para*-*n*-octylphenyacetylene was stereoregularly polymerised using [Rh(norbornadiene)Cl]$_2$ in ethanol at -20 °C and 25 °C to afford yellow and orange polymers, Poly(**Y**) and Poly(**O**), respectively, in high yields. Poly(**Y**) transformed into red polymer, Poly(**R**), upon heating to 100 °C. The XRD patterns of Poly(**Y**) revealed

that it has a *hexagonal* columnar crystal structure comprising *cis-cisoid helices*, i.e., *contracted helices*, called ^{Hexa}Poly(**Y**)^{CC}. Furthermore, heating ^{Hexa}Poly(**Y**)^{CC} up to 100 °C induced a solid phase transformation to the red polymers, ^{Tetra1}Poly(**R**)^{CC} and ^{Tetra2}Poly(**R**)^{CT}, respectively. Moreover, we revealed that the ^{Hexa}Poly(**Y**)^{CC} and ^{Tetra2}Poly(**R**)^{CT} have ~~a~~ bend *n*-octyl side chains using the solid state ^{13}C CP-MAS NMR method.

This study described new helical polyacetylenes which are composed from stretched helix and/or contracted helix. The color of the polyacetylenes was attributed to the geometrical structure and higher order structure, i.e., helical pitch width and the increment of intramolecular π-stack order in the polymer chain. Furthermore, we revealed that the columnar polymers comprising of the helical chains have two crystals phase, i.e., hexagonal crystal and tetragonal crystal. And we also revealed that the helical pitch and crystal structure could can be controlled by the heat-treatment. Thus, this study described important chemical and physical features of a *helical* π-conjugated polymer, that will be developed as a new class of advanced materials and /or molecular materials near future.

List of Publications

1. Asahi MOTOSHIGE, Yasuteru MAWATARI, Yoshiaki YOSHIDA, Chigusa SEKI,

Haruo MATSUYAMA, and Masayoshi TABATA, 「Irreversible Helix Rearrangement from Cis-transoid to Cis-cisoid in Poly(*p*-*n*-hexyloxyphenylacetylene) Induced by Heat-treatment in Solid Phase」, *J. Polym. Sci., Part A: Polym. Chem*., **2012**, 50, 3008-3015.

2. Asahi MOTOSHIGE, Yasuteru MAWATARI, Ranko MOTOSHIGE, Yoshiaki YOSHIDA, and Masayoshi TABATA, 「*Contracted Helix* to *Stretched Helix* Rearrangement of an Aromatic Polyacetylene Prepared in *n*-Hexane with [Rh(norbornadiene)Cl]$_2$-trietylamine Catalyst」, *J. Polym. Sci., Part A: Polym. Chem*., **2013**, 51, 5177-5183.

3. Asahi MOTOSHIGE, Yasuteru MAWATARI, Yoshiaki YOSHIDA, Ranko MOTOSHIGE, and Masayoshi TABATA, 「Synthesis and Solid State *Helix* to *Helix* Rearrangement of Poly(phenylacetylene) Bearing *n*-Octyl Alkyl Side Chains」, *Polym. Chem.*, **2014**, 5, 971-978.

4. Yoshiaki YOSHIDA, Yasuteru MAWATARI, Asahi MOTOSHIGE, Ranko MOTOSHIGE, Toshifumi HIRAOKI, Manfred WAGNER, Klaus MÜLLEN, and Masayoshi TABATA, 「Accordion-like Osillation of Contracted and Stretched Helices of Polyacetylenes Synchronized with the Restricted Rotation of Side Chains」, *J. Am. Chem. Soc.,* **2013**, 135, 4110-4116.
5. Yoshiaki YOSHIDA, Yasuteru MAWATARI, Asahi MOTOSHIGE, Ranko

MOTOSHIGE, Toshifumi HIRAOKI, and Masayoshi TABATA, 「Helix Oscillation of Polyacetylene Esters Detected by Dynamic ^{1}H NMR, IR, and UV-vis Methods in Solution」, *Polym. Chem.*, **2013**, 4, 2982-2988.

6. Ranko MOTOSHIGE, Yasuteru MAWATARI, Asahi MOTOSHIGE, Yoshiaki YOSHIDA, Takahiro SASAKI, Hiroaki YOSHIMIZU, Tomoyuki SUZUKI, Yoshiharu TSUJITA, Masayoshi TABATA, 「Mutual Conversion between *Stretched* and *Contracted Helices* Accompanied by a Drastic Change in Color and Spatial Structure of Poly(phenylacetylene) Prepared with a $[Rh(nbd)Cl]_2$-Amine Catalyst」, *J. Polym. Sci., Part A: Polym. Chem*., **2014**, 52, 752–759.

Acknowledgements

This thesis presents the studies which the author has carried out from 2009 to 2013 at

Department of Chemical and Materials Engineering, Muroran Institute of Technology.

The author would like to express my gratitude to Professor Masayoshi Tabata for his continuous guidance and critical suggestions throughout this study.

The author is also grateful to Professor Haruo Matsuyama and Professor Hiroto Nakano for their helpful advices. The author is deeply grateful to Dr. Yasuteru Mawatari for his constant guidance, interesting discussion and encouragement.

The author is grateful to Professor Toshifumi Hiraoki (Hokkaido University) for NMR measurements and advice, Mr. Yoshikazu Sadahiro for X-ray diffraction measurement and discussion.

The author is grateful to Professor Klaus Müllen and his Lab. members (Max-Planck Institute for Polymer Research in Germany) and Professor Roberto Lazzaroni and his Lab. members (University of Mons in Belgium) for giving me to useful opportunities and interesting discussion.

The author thankful to member of Tabata Lab. members; Dr. Yoshiaki Yoshida, Dr. Takahiro Sasaki Ms. Ranko Motoshige and Matsuyama Lab. members for spending me useful and enjoyable research activities.

Finally, the author is deeply grateful to my family for everything.

March 2014

Asahi Motoshige